UNIVERSITY OF CALIFORNIA, SAN DIEGO

The Role of UPF Proteins in Nonsense-Mediated Decay and in Neurogenesis

A thesis submitted for the partial satisfaction of the

requirements for the degree Master of Science

in

Biology

by

Matthew Krause

Committee in Charge:

Professor Miles Wilkinson, Chair
Professor Jens Lykke-Andersen, Co-chair
Professor Andrew Chisholm

2014

This thesis of Matthew Daniel Krause is approved, and it is acceptable in quality and form for publication on microfilm and electronically:

_____

_____

Co-Chair

_____

Chair

University of California, San Diego

2014

Dedication

I would like to dedicate this work to my friends and family who helped me to accomplish everything I have done.

Table of Contents

List of Figures

Acknowledgements

I would like to thank everyone in the Wilkinson lab for all of their contributions, individual and collective.

I would like to thank Marcy Richardson for being my first mentor in the lab, and teaching me the skills to be an excellent researcher.

I would like to thank Heidi Cook-Andersen for recommending me for graduate school and encouraging me to broaden my horizons.

I would like to thank Eleen Shum for giving me a great project and an opportunity to work alongside her in the lab.

I would also like to thank Miles Wilkinson who tirelessly works to make this lab great, for his input, all of his help in writing this thesis, and being an excellent mentor.

ABSTRACT OF THE THESIS

The Role of UPF3 Proteins in Nonsense-Mediated Decay and in Neurogenesis

by

Matthew Daniel Krause

Master of Science in Biology

University of California, 2014

Professor Miles Wilkinson, Chair

Professor Jens Lykke-Andersen, Co-chair

Nonsense-mediated RNA decay is an evolutionarily conserved RNA quality control pathway designed to protect cells from genetic aberrances as well as to modulate normal gene expression during development. Many proteins have been identified that function in NMD, including UPF3B, which is encoded by an X-linked gene that causes intellectual disability when mutated in humans. In this study, I examined the role of both *UPF3B* and its autosomal paralog, *UPF3A*, in a well-established system for studying neural development: the olfactory epithelium.

Using knockout mouse models deficient in UPF3A, UPF3B, or both, I obtained evidence as to the molecular and physiological roles of these factors in the development of olfactory sensory neurons. I found that conditional loss of UPF3A in OSNs resulted in a shift in OSN markers suggestive of a depletion of OSN stem cells and an over-accumulation of mature OSNs. This provided evidence that UPF3A controls the balance of OSN stem cell renewal and differentiation. Examination of NMD substrates in *Upf3a*-conditional KO (cKO) OE *in vivo* revealed that UPF3A has the opposite function as UPF3B – it represses NMD. Consistent with the opposing roles of UPF3A and UPF3B, genetic disruption of both these factors partially rescued defects present in single mutants. This supports a model in which UPF3A and UPF3B together form a molecular rheostat that controls the magnitude of NMD and thereby the stability of transcripts crucial for normal neural development. These results implicate the UPF3 proteins as potentially useful therapeutic targets to correct some neuro-developmental disorders.

I:

Introduction

Nonsense-mediated RNA Decay

Nonsense-mediated RNA decay (NMD) was initially discovered as a post-transcriptional quality control mechanism that targets aberrant transcripts containing premature termination codons (PTCs) for degradation to preclude the synthesis of truncated and potentially deleterious proteins (Huang *et al.* 2012, Hwang *et al.* 2011, Nicholson *et al.* 2010, Rebbapragada *et al.* 2009). The best-established NMD-inducing context is when a stop codon is upstream of at least one exon-exon junction. This allows a set of NMD-enhancing proteins recruited near exon-exon junctions—collectively called the exon-junction complex (EJC)—to avoid being displaced by translating ribosomes (Huang and Wilkinson, 2012). The remaining EJC is then able to interact with UPF1, an NMD factor that accumulates in the 3' UTR region (Hogg *et al*. 2010), which then triggers rapid mRNA decay by mechanisms that are still being resolved (Chang *et al.* 2007, Kervestin *et al.* 2012, Schoenberg *et al.* 2012). Through further investigation, NMD has also been shown to also target normal transcripts with features such as a long 3' untranslated region (UTR), an intron in the 3' UTR, or an upstream open reading frame (uORF). Microarray studies of NMD-deficient mouse models and cell lines have shown evidence of NMD being directly, or indirectly responsible for regulating as little as 3% and as much as 15% of the normal transcriptome (Chan *et al.* 2007, Guan *et al.* 2006, He *et al.* 2003, Lelivelt *et al.* 1999, Mendell *et al.* 2004, Ramani et al. 2009, Rehwinkel *et al.* 2005, Wittmann *et al.* 2006). This implicates NMD as not only a quality control pathway but also a regulator of normal gene expression, the latter of which raises the possibility that it is a regulator of normal cellular

development. Indeed, my study focuses on NMD's regulatory role in cellular development.

The NMD complex is composed of up-frameshift (UPF) proteins that are critical for the recognition and termination of PTC-containing transcripts (Lykke-Andersen *et al.* 2000, Serin *et al.* 2001, Kunz *et al.* 2006). The major NMD factors investigated in this study are the UPF3A and UPF3B proteins. These two proteins are paralogous, meaning they arose through duplication in the genome and have persisted throughout evolution. Both UPF3A and UPF3B are ubiquitously expressed, but exhibit tissue-specific differences in their level of expression. UPF3A is encoded by an autosomal gene, while UPF3B is encoded by an X-linked gene. The UPF3B protein can destabilize and thus lower the level of the UPF3A protein, without changing its level of transcription (Chan *et al.* 2009). As a result, loss of UPF3B leads to an increase of UPF3A protein expression.

UPF3A and UPF3B have long been assumed to have redundant roles, as both bind to UPF2 as well as the Y14 and MAGOH components of the EJC (Kadlec *et al.* 2004, Melero *et al.* 2012). Experiments using a tethering assay to bind UPF3A or UPF3B to the 3' of a reporter mRNA showed that UPF3A was not as effective in eliciting NMD as UPF3B (Lykke-Andersen *et al.* 2000). As a result, UPF3A has been generally regarded as a weak NMD factor and been largely ignored since these tethering experiments were reported. The main purpose of my study is to investigate whether UPF3A is important and to decipher its relationship with UPF3B.

NMD factor proteins have been shown to be physiologically relevant through generation and study of mouse knock out (KO) models. Complete loss of different factors involved in the NMD pathway, including UPF1, UPF2, UPF3A, and the serine/threonine-protein kinase (SMG1), all produce an embryonic lethal phenotype (Hwang *et al.* 2011, Shum *et al*., manuscript in preparation). These data suggest that many NMD factors, including UPF3A are essential for development events and embryonic viability. Interestingly, complete loss of UPF3B seems to be the only exception in that it does not result in embryonic lethality (Huang *et al.* manuscript in preparation). Instead, mutations in *UPF3B* in humans causes intellectual disability and is associated with mental disorders such as autism, attention deficit hyperactivity disorder, and schizophrenia (Tarpey *et al.* 2007, Addington *et al.* 2011, Laumonnier *et al.* 2010, Nguyen *et al.* 2012, Szyszka *et al.* 2012, Nguyen *at al.* 2013). Monogenic mutations of *UPF3B* are sufficient to cause neurodevelopmental defects suggesting *UPF3B* is required for neurogenesis; however; is not necessary for embryonic viability as these patients survive and reach adulthood. Together, these studies suggest that UPF3A and UPF3B serve distinct functions, and that both UPF3A and UPF3B do not simply have redundant roles for *in vivo* development. My study investigates the role of these two proteins in neurogenesis in order to elucidate their physiological roles in cellular development, as well as to understand how their roles in the NMD pathway may shape and influence downstream mechanisms that dictate and regulate cellular differentiation.

Signaling Pathways Regulated by NMD

NMD has been shown to promote transforming growth factor (TGF-β) signaling events that are crucial for cellular development and specifically neurogenesis (Lou *et al.* 2014). TGF-β signaling promotes an undifferentiated cell state. By degrading mRNA encoding proteins that would otherwise inhibit TGF-β signaling, NMD promotes the stem-like state. The developmental cue for neural stem cells to differentiate is when NMD is inhibited through the down-regulation of UPF1 by a microRNA, mir128. Understanding the underlying molecular mechanisms driving cellular differentiation is vital to illuminating NMD's biochemical role.

Another signaling pathway regulated by NMD is the unfolded protein response (UPR), a pathway critical for endoplasmic reticulum (ER) homeostasis. The UPR is activated in response to misfolded proteins in the ER; it deals with misfolded proteins through recruitment of chaperone proteins, halting translation, degrading misfolded proteins, or having the cell undergo apoptosis. UPR positively feedbacks NMD by up-regulating NMD factors in response to ER stress (Sakaki *et al.* 2013, Oren *et al.* 2014, Karam *et al.* manuscript submitted). When NMD is inhibited, this leads to an increase in UPR activity, which will further inhibit NMD activity, a positive feedback loop that greatly amplifies the UPR. The UPR has also been implicated in olfactory neurogenesis, specifically for the selection of olfactory receptors (ORs), which I will discuss in the next section (Dalton *et al.* 2013).

Investigation of the role of NMD in regulating these pathways is critical to connecting genetics to downstream phenotypic effects. Cellular development will be modulated by TGF-β signaling and the UPR, among other signaling pathways.

Regulation of these signaling pathways is controlled by NMD, putting NMD at the center of a large network of mechanisms and pathways. Control of NMD by its factors will then lead to elucidation of the molecular and physiological roles that each individual protein plays.

NMD in Neurogenesis

Mutations in UPF3B have been shown to cause a neural deficient phenotype. In humans, UPF3B-linked intellectual disabilities were discovered through pedigree studies of families with inherited forms of intellectual disability. An interest in understanding the role of mutations in the *UPF3B* gene in inheritable forms of intellectual disability has lead to the generation of the UPF3B knockout mouse model (Huang *et al.* manuscript in preparation). Depletion of UPF3B (using RNA interference [RNAi]) has been shown to result in loss of neural progenitor cells, less neurite (axons or dendrites of immature neurons) density, and result in less mature neural cell density in the hippocampus (Jolly *et al.* 2013). These abnormalities have been identified as underlying developmental abnormalities resulting in reduced cognitive capabilities associated with neurological deficiencies and disorders. The *Upf3b-null* mice have specific defects that reflect some of the defects seen in humans such as problems with: learning and memory (learning to avoid harmful stimuli, fear conditioned learning), a specific sensory-motor defect (pre-pulse inhibition, which measures impairment of the startle response), and major deficits in olfactory neurogenesis, including reduced numbers of both olfactory stem cells and sensory neurons (Huang et al. manuscript in preparation).

These data implicate NMD and specifically UPF3B as being required for normal neurogenesis.

Interestingly, many of the same studies that implicated UPF3B loss as the etiology for inherited forms of intellectual disability, identified even more patients with gains or losses of UPF3A (Nguyen *et al.* 2012). These patients, while not studied as comprehensively as the UPF3B patients, had a phenotype of neural tube defects. While UPF3A and UPF3B have long been assumed to be redundant, loss of either protein results in a unique disease-related phenotype. In order to elucidate the relationship between these two proteins and their physiological roles, our lab generated a mouse deficient in UPF3A. Characterizing this mouse model and UPF3A's role in development are the primary foci of study for this report.

The chosen physiological model for this study is the mouse olfactory epithelium (OE). The olfactory epithelium serves as an ideal model for neurogenesis (Whitman *et al.* 2009, Haehner *et al.* 2011, Rupp *et al.* 2010). The brain as a whole is very intricate for experimentation purposes as there are many different cell types in each region. The OE has only one cell type allowing for a simpler model of neurogenesis. The OE is also one of only a few regions in the nervous system to undergo adult neurogenesis that allows for experimentation on adult animals as opposed to embryos. Olfactory neurogenesis begins with the horizontal basal cells (HBCs), which are the stem cells in the basal layer of the OE (DeMaria *et al.* 2010). HBCs differentiate into the globular basal cells (GBCs), the progenitor cells. The GBCs then develop into the immature olfactory sensory neurons (iOSNs) that will become the mature olfactory sensory neurons (mOSNs).

Each mOSN has only one olfactory receptor out of a total repertoire of around 1,000 genes in the human genome, and 1,500 in mice (Zhang *et al.* 2002). These olfactory receptors protrude into the lumen of the OE to detect odarants. The axons of mOSNs extend all the way to the olfactory bulb that lies on the rostral part of the brain. Neurons expressing a common olfactory receptors converge to form glomeruli on the olfactory bulb and are thought to contribute to odor coding (Bozza *et al.* 2009). This results in segregation of the olfactory receptors by type and also by class relative to position on the olfactory bulb (Tsuboi *et al.* 2006).

The OE is unique from other parts of the central nervous in system in that neurogenesis continues well into adulthood. mOSNs can be damaged and lost, which forces the HBCs that reside in the basal layer of the OE to divide, differentiate, and repopulate the OE with mOSNs (Whitman *et al.* 2009, Iwai *et al.* 2008, Leung *et al.* 2007). Chemical ablation of the cells in the OE allows for regeneration to be observed in adult mice by removing all of the neurons (Piras *et al.* 2003). This method leaves behind only the stem cells that are forced to divide in order to repopulate the OE with more neurons. This model of neurogenesis allows for development to be studied in a choreographed and synchronized manner in adult animals using a regeneration model initiated by chemically ablating all OSNs except for the HBCs.

In unpublished work from the Wilkinson laboratory, the *Upf3b-null* mouse has been shown to have olfactory defects. As with other neuronal defects in UPF3B deficient mice, the OE has a decrease in the number of HBC and mOSNs, implicating NMD and specifically UPF3B as essential components to normal

olfactory neurogenesis. This can be partially explained by mis-regulation of the signaling pathways governed by NMD such as UPR and TGF-β, which were previous mentioned. For example, the UPR has been reported to be activated in iOSNs as they begin to express an OR out of a repertoire of over 1,500 genes (Dalton *et al.* 2013). The UPR is the repressed once the OR selection has been made through a negative feedback process. Applying the information from these previous studies I can hypothesize that if UPF3A acts redundantly with UPF3B, then the same defects should be observed. In the event that UPF3A is not redundant, it is still very likely to observe different defects as many processes regulated by NMD are still required in olfactory neurogenesis.

Study of the OE is directly relevant to the study of other neurological disorders. As previously mentioned, the OE is a very simple model in that there is only one type of neuron, as opposed to heterogeneous mixtures of neuronal cell types in the regions of the brain. Olfactory defects are commonly found in and are often used as a predictor for humans with central nervous system disorders making this model directly relevant and applicable to the development of other neuronal populations.

Implications and Clinical Relevance

As discussed above, UPF3B deficiency has been associated with a variety of mental disorders. What remains unclear is whether UPF3B loss or UPF3A up-regulation is the underlying cause of the phenotype. If future experiments show that UPF3A loss is actually beneficial to an organism, UPF3A would be an ideal

therapeutic target to the UPF3B deficient patients. Understanding the process of neurogenesis will give more understanding to the etiology of neural-related diseases. By This understanding of the underlying cause of these disorders will allow for development of treatment that could target UPF3A or UPF3B in patients and help to treat their disorders.

My experiments seek to illuminate to physiological roles of UPF3A and UPF3B in neurogenesis. Concurrently, these experiments will elucidate the relationship between gene paralogs UPF3A and UPF3B as NMD factors. This information will allow for understanding of how the NMD pathway influences normal neuronal development.

II:

Results

UPF3A is a NMD Repressor

In order to understand the role of UPF3A in NMD *in vitro*, I began experimentation by using an shRNA to knock down *Upf3a* in P19 cells, a mouse embryonic teratoma cell line that endogenously expresses UPF3A. Knockdown experiments with other NMD factors such as *Upf1*, *Upf2*, and *Upf3b* result in a higher expression of NMD targets, as fewer of the transcripts are being degraded through the NMD pathway (Huang *et al.* 2011). Surprisingly, in response to knockdown of *Upf3a*, there was a decreased level of NMD targets, instead of an increase as seen with other NMD factors (Figure 1A). If increased expression of NMD targets indicates weakened NMD, then conversely a down-regulation of NMD substrates would indicate stronger NMD. This suggested that there was increased decay of NMD and thus greater NMD activity as a result of *Upf3a* knockdown.

To observe if UPF3A was directly responsible for the stabilization of these transcripts I transfected P19 cells with either shRNA or an expression vector for *Upf3a*. In addition, I used a dual NMD reporter system to measure the ratio of PTC−/PTC+ mRNAs to quantify NMD activity. Twenty-four hours post-transfection the cells were treated with Actinomycin D that binds DNA at the transcription initiation complex and prevents elongation by RNA polymerase to stop transcription. Performing a time course experiment allowed me to observe the half-lives of different RNAs and see if stability was affected by knockdown or overexpression of *Upf3a*. Using the PTC+/PTC- reporter system, I was able to see a decrease in reporter mRNA over time in the *shUpf3a* sample, as seen by the

decreasing ratio of PTC+/PTC- indicating stronger NMD (figure 2A). There was little to change in the PTC+/PTC- ratio in response to *Upf3a* overexpression. In response to *Upf3a* knockdown, the mRNA transcripts were destabilized. Likewise, in response to *Upf3a* overexpression, the transcripts were more stable, relative to the control (figure 2B). These results were unexpected as knockdown of *Upf3a* resulted in stronger NMD, and *Upf3a* overexpression resulted in weaker NMD, which is the complete opposite result observed when any other NMD factor that has been knocked down or overexpressed (Huang et al. 2011, Chan *et al.* 2007, Lou *et al.* 2014).

UPF3A is Functionally Conserved

The UPF3A/UPF3B protein paralog pair is evolutionarily ancient and exists in all vertebrates (Wittkopp *et al.* 2009). While this paralog pair is conserved, each of these two paralogs have diverged considerably in sequence over evolutionary time. To test if the human form of UPF3A was able to show the same effects as the mouse form of UPF3A, I transfected different dosages of the human form of UPF3A into mouse P19 depleted of mouse UPF3A by transfecting a *shUpf3a* plasmid. Knockdown alone of *Upf3a* lead to a PTC/PTC- ratio greater than 1.0, indicating stronger NMD. Increasing amounts of the hUPF3A led to NMD repression as seen by the decreasing PTC+/PTC- ratio back down to one indicating NMD inhibition (figure 3A). I performed a similar experiment by titrating different amount of human UPF3A into P19 cells with the NMD reporter construct.

In response to this I observed a negative correlation between the amount of human UPF3A added and NMD reporter activity (figure 3B). As the amount of hUPF3A increased, the strength and PTC-/PTC+ ratio decreased and showing evidence that NMD was more and more inhibited.

UPF3A Requires Amino Acids Encoded by Exon 4 to Repress NMD

In order to determine the parts of the UPF3A protein required for NMD inhibition, I used several hUPF3A mutant clones to perform titration experiments, as I did above with full-length hUPF3A. UPF3A has been previously shown to interact with Y14 and MAGOH of the EJC and UPF2 (Kadlec *et al.* 2004). Both of the clones that are unable to bind UPF2 and Y14 still showed the same repressive capabilities as hUPF3A (figure 4A, B). The only exception was the UPF3A-ΔExon4 (E4) isoform, which did significantly repress NMD (figure 4C). These data show that UPF3A requires the amino acids encoded by E4 to inhibit NMD.

With all of these mutants I performed a rescue experiment by transfecting *shUpf3a*, one of the hUPF3A clones, and the NMD reporter. The *shUpf3a* alone results in a higher PTC-/PTC+ ratio, and this is brought down by UPF3A's repressive function (figure 4D). All of the clones with the exception of the hUPF3A-ΔE4 was able to counter-act the function of the *shUpf3a*. This results confirm that UPF3A is able to act as an NMD repressor and that it requires the amino acids encoded by E4 for this function.

OE Defects Caused by Loss of One Copy of *UPF3A* or Complete Loss of *UPF3B*

In order to study UPF3A's role *in vivo*, floxed-*Upf3a* mice were generated by Eleen Shum, a PhD student in the Wilkinson laboratory. As stated in the Introduction, her unpublished studies with these *Upf3a*-mutant mice revealed that complete loss of UPF3A is embryonic lethal. Therefore, I performed my initial experiments using heterozygous (*Upf3a*$^{+/-}$) mice.

A measure of a mouse's ability to smell is to take its weight at weaning (Logan *et al.* 2013). The mice nurse until around P21, and then they start to feed themselves. The pups rely on their olfaction in order to feed, and thus a pup with olfactory defects will be smaller as it is unable to feed as much as its litter-mates. By normalizing all of the pups to their wild-type littermates of the same gender, I plotted a normalized graph of mouse weight at the time of weaning. *Upf3b-null* (*Upf3b*$^{-/*}$) mice had a 25% reduction in body weight relative to wild type (figure 5A). This suggests that complete loss of Upf3b causes a partial olfactory defect, a conclusion supported by unpublished evidence from Eleen Shum, a PhD student in the Wilkinson laboratory. I found that *Upf3b*$^{+/-}$ females were only 10-15% smaller than control mice, but this reduction was statistically significant. The *Upf3a*$^{+/-}$ mice had no appreciable difference in body weight relative to control mice, indicating that they do not possess an anosmia phenotype, unlike *Upf3b*-mutant mice.

In order to track olfactory neurogenesis, I extracted the OE at different time points during postnatal development and analyzed OE RNA using qPCR. *Krt5* and

Icam1 were used to as markers to track and quantify the population of HBCs in the OE. *Upf3a*$^{+/-}$ mice had ~40-50% reduction in HBC markers from four to twelve weeks after birth (Figure 4B). Meanwhile, the mOSN marker *Adcy3* was around two-fold higher relative to wild type (Figure 5C). This suggested that haplo-insufficiency of *Upf3a* may cause a stem cell defect that leads to increased differentiation of mOSNs.

To more completely investigate and characterize olfactory neurogenesis in the *Upf3a*$^{+/-}$ mice, I chose to also observe the levels of OSN protein markers and cell morphology. To compare relative quantities of protein markers in the mouse OE, I performed a western blot using proteins isolated from wild type and *Upf3a*$^{+/-}$ mouse OE tissues. I used an antibody for p63 again to observe the total amount of p63 protein to compare the HBC population between the *Upf3a*$^{+/-}$ and wild type mice. After quantification, it appears as though there was more p63 in the *Upf3a*$^{+/-}$ OE than in the control, but the increase is not statistically significant (figure 6A, B). This does not agree with my qPCR data, which showed a reduction in HBC markers in the *Upf3a*$^{+/-}$.

In order to measure any changes in the mOSN population in the OE, I used an antibody for OMP that is a marker for mature neurons. The Western blot showed that there was a significant increase in the amount of OMP protein in the *Upf3a*$^{+/-}$ mice (Figure 6A, B). This agreed with the qPCR data, which showed an increase in mOSN markers.

To further test changes in cell population in response to UPF3A haploinsufficiency I looked at the cell morphology and protein markers. Using fluorescence microscopy, I looked at the HBCs by probing for p63 and counted the cells. While the RNA level showed that the reduction of HBCs was as low as 50% compared to wild-type, the difference in p63+ cells compared to wild type was only 15-20% (Figure 7A, B). As previously mentioned, the western blot showed no significant change which does not agree with either the qPCR data or the histological staining. As to why there is a discrepancy between the RNA and protein markers is unclear, but at least two of the three tests agree that there is a decrease in HBCs, albeit very subtle.

To determine the effect of Upf3a haplo-insufficiency on OSN proliferation I used an antibody against the proliferation marker, Ki67 (Scholzen *et al.* 2000). What I observed in the *Upf3a*$^{+/-}$ OE was an increase in Ki67^{+} cells relative to control OE (figure 7A, B). This effect was particularly prominent in the middle layers of the OE as opposed to the basal layer (figure 7A, B). This raised the possibility that there are more proliferating differentiating cells in the *Upf3a*$^{+/-}$ mouse OE compared to control OE (Figure 7A). Differentiation and proliferation of OSN precursor cells occur simultaneously as a result of asymmetrical division from stem or progenitor cells (Mackay *et al.* 1991). The increased mOSN markers, coupled with the increase in proliferation, suggest that in response to UPF3A haploinsufficiency the HBCs and/or GBCs are stimulated to divide. The reduction of HBCs can be seen as a consequence of increased proliferation and differentiation in response to UPF3A loss. The qPCR, western blot, and histological

staining agree that there is a shift in the *Upf3a*$^{+/-}$ cell population to more differentiated cells. Whether or not this causes a reduction in the HBCs, is unclear, but this could occur as a consequence of increased division leading to stem cell exhaustion, or improper division leading to stem cell loss.

I considered the possibility that some of these *Upf3a*$^{+/-}$ defects were ameliorated by compensation from UPF3B. In previous studies, UPF3A protein was shown to be significantly unregulated when UPF3B is lost because UPF3B leads to UPF3A protein instability (Chan *et al.* 2009). Transcription remains unchanged, but the UPF3B protein leads to the destabilization of UPF3A. I sought to determine if the converse occurs – does depletion of UPF3A causes an increase in UPF3B levels? According to the western blot performed, loss of UPF3A has no observable effect on the protein expression of UPF3B (figure 6A, B).

One of the benefits of studying neurogenesis in the OE is the ability of the OE to repopulate itself with neurons following chemical ablation with methimazole, a cytochrome P450 inhibitor that causes the cells of the OE to die and subsequently force the HBCs to divide in response to the damage (Mackay *et al.* 1991, Fletcher *et al.* 2011). Mice were administered 5 Mg/ml of methimazole via intraperitoneal injection. After injection the mice were allotted time for recovery and then the mice were sacrificed and the OE was harvested. For this experiment, the mice were left one week to recover one week following injection. I sacrificed the mice, extracted the OE, then embedded and sectioned the tissues for observation. I measured the thicknesses of the OE to compare the ability of the different

genotypes of mice to recover following methimazole treatment. I found that only *Upf3b*$^{-/*}$ mice had a defect in repopulating the OE with mOSNs (figure 8A). *Upf3a*$^{+/-}$ mice exhibited normal OE thickness, indicating no gross defects in the OE, at least in this regeneration assay.

OE Defects in *Upf3a* cKO mice

The above experiments were performed with *Upf3a* heterozygous mice and thus only determined defects resulting from reducing the dose of UPF3A by one-half. To determine the effect of complete loss of *Upf3a*, I generated a conditional knockout of *Upf3a* specific to OSNs and their precursor cells. To accomplish this, I used *Krt5*-Cre driver mice, which express tamoxifen-inducible Cre recombinase in HBCs (Tarutani et al. *1997*). This allowed me to generate *Upf3a* conditional knockout (cKO) that lack UPF3A in HBCs and all subsequent generations of OSNs, including mOSNs.

In order to test the expression characteristics of the *Krt5*-Cre mice, I bred them with *Rosa26-LacZ* reporter mice. The *Krt5* promoter is expressed in the OE and not in other parts of the brain and thus that is the staining pattern of lacZ that should be observed. One week following methimazole injection, mice were sacrificed and the OEs were subjected to staining using X-gal. I observed staining only in the OE and not in other regions of the brain such as the olfactory bulb or elsewhere, confirming that the conditional knockout was in fact specific to the OE (supplemental figure 1). *Krt5* is also expressed in stem cells in the skin (Fletcher

et al. 2011), but I did not take any skin samples to test for lacZ expression in the skin.

Once I generated *Upf3a*-cKO mice, I determined whether they had the same, different, or stronger phenotype compared to the *Upf3a*$^{+/-}$ mice. Using RNA extracted from the OEs extracted from *Upf3b*$^{-/*}$ and *Upf3a-cKO* mice bred in parallel, I performed qPCR to observe the relative quantities of the different olfactory cell populations. As with my above experiments with *Upf3b*$^{-/*}$ mice, I observed a reduction in both HBC and mOSN markers (figure 9A). This confirmed previous studies done by Eleen Shum and supports the evidence I had already obtained showing that these mice have an olfactory defect due to fewer neural stem cells, as well as fewer mature neurons. The *Upf3a*$^{+/-}$ mice had a profile of marker expression consistent with a shift in the OE cell population towards more differentiation, and thus I wanted to measure if the effect was more pronounced in the *Upf3a-cKO* mice. Following two weeks induction of tamoxifen to drive Cre recombinase expression, I sacrificed the mice and isolated RNA from the OE and performed qPCR. As seen previously in the *Upf3a*$^{+/-}$ mice, the HBC markers were reduced in level (~50%), but unlike the *Upf3a*$^{+/-}$ mice, this was only a trend; it was not statistically significant (figure 9B). The same effect was observed in the *Upf3a-cKO*. This was somewhat surprising as one would normally expect a stronger phenotype in a full knockout as compared to one that is only heterozygous. The mOSN markers, however were much higher than I had seen in the *Upf3a*$^{+/-}$ mice, with 4- and 16-fold increase in *Adcy3* and *Gng13*, respectively (figure 9B). While I have not directly counted the number of mOSNs, this data suggests that these

Upf3a-cKO mice have many more mOSNs than either *Upf3a*$^{+/-}$ mice or control mice. Both the *Upf3a*$^{+/-}$ and *Upf3a-cKO* show a very similar olfactory phenotype. While neither has an obvious weaning weight deficit indicative of an olfactory defect (figure 5A), both show decreased HBC markers, and increased mOSN markers indicating a possible shift in the OE cell population more towards the more differentiated state.

UPF3A Represses NMD in the OE

NMD has been previously been shown to regulate TGF-β signaling and shape the UPR (Lou *et al.* 2014, Karam *et al.* submitted). Many of the factors in the TGF-β and UPR pathways are encoded by mRNAs that are targeted by NMD. I chose many of these mRNAs to not only test the relative strength of NMD in response to UPF3A or UPF3B deficiency, but also to serve as possible links between the genetics of the mice and the observable phenotypes such as the intellectual disabilities and neural deficiencies seen in the *Upf3b*$^{-/*}$ mice. These phenotypes which indicate improper neurogenesis are known, but it is important to link the whole pathway from genotype to the cellular events that give rise to the observed phenotype.

From the RNA extracted from *Upf3b*$^{-/*}$ and *Upf3a-cKO* mice, I performed more qPCR reactions to measure relative quantities of different NMD targets to measure NMD strength. In the *Upf3b*$^{-/*}$ mice, I observe up-regulation in most NMD target RNAs (figure 10A), indicating weakened NMD, which has been reported in

previous studies (Huang *et al.* 2011). For example,, there was significant up-regulation of the mRNAs encoding the TGF-β associated factors *Smad5* and *Smad7*, both of which have previously been shown to encode NMD target transcripts; the latter of which functions with NMD in neural differentiation (Lou *et al.* 2014). Also up-regulated were *Atf4* and *Chop* mRNA, which are NMD target transcripts that encode UPR components (Karam *et al.* 2013). Interestingly, the NMD target transcript, *Ire1α* mRNA, was *not* upregulated, which differs from its response to loss or depletion of UPF3B in HeLa cells and liver (Karam *et al.,* submitted). The OE may have cell type-specific factors that prevent *Ire1* mRNA from being degraded by NMD. XBP1-spliced (S) mRNA, whose generation is catalyzed by IRE1α (Yoshida *et al.* 2001), was also not upregulated, confirming that *Ire1α* mRNA levels were not upregulated. While XBP1S is not an NMD substrate, it has been tested and included in the study in order to show UPR activation.

In striking contrast to the *Upf3b*$^{-/*}$mice, the *Upf3a-cKO* mice had consistent and significant down-regulation of all NMD substrates (figure 10B). This provided more evidence of stronger NMD in response to loss of UPF3A. Most targets are down-regulated 80-90%, while *Upf1* mRNA was reduced by around 50% (figure 10B). The reduction in *Upf1* mRNA level is consistent with the previous finding that it is targeted for NMD (Huang *et al.* 2011, Yepiskoposyan *et al.* 2011), but was surprising given that UPF1 is essential for NMD (Schweingruber *et al.* 2013). Given that *Upf3a-cKO* mice have *stronger* NMD than control mice, the reduction

in *Upf1* mRNA levels in these mice suggests that UPF1 is not rate-limiting for NMD in the OE.

Non-coding RNAs are Expressed Independently of UPF3A and UPF3B

Of all the NMD substrates I tested, the only two that did not exhibit significant down-regulation in the OE of *Upf3a*-cKO mice were *Gas5* and *Snord22* RNA (figure 11A, B). This is interesting in light of the fact that these are both long non-coding RNAs (Chinen *et al.* 2012, Tycowski *et al.* 1996). They were also not significantly altered in level in *Upf3b*-null and *Upf3a/Upf3b* double-mutant mice (figure 11A, B). These data suggest that the ability of NMD to degrade long non-coding RNAs may be independent of the UPF3 proteins in the OE. Whether this is novel feature of the OE or of the UPF3 proteins remains for future studies.

Tissue Specific Effects of UPF3A

The majority of my study focused on the role of UPF3A in the OE. To examine tissue specificity, I elected to investigate the effect of loss of UPF3A in other tissues. I chose to also analyze the heart, brain, and spleen. The heart and brain have fairly high expression of both UPF3A and UPF3B (but not nearly as high levels of UPF3A as the testis), while the spleen has very little of either (Wai-Kin Chan, unpublished data). I took tissue samples from Upf3a$^{+/-}$ mice and isolated the RNA for qPCR analysis. What I found was each tissue has a rather unique

expression profile of different NMD targets (figure 12 A-C). In the heart, I saw significant down-regulation of *Ire1α* and *Snord22* mRNA, and significant up-regulation in *Atf4, Xbp1s,* and *Atp1a2* mRNA. In contrast, in the brain there was very different results: *Atf4* and *Ire1α* were significantly down-regulated and *Atp1a2* and *Snord22* were up-regulated. In the spleen the relative quantities of NMD substrates were also different, with *Atf4*, *Ire1α*, and *Xbp1s* all being down-regulated and *Smad7* and *Atp1a2* being up-regulated.

Olfactory and NMD Defects are Suppressed in *UPF3A/UPF3B* Double Mutants

With the evidence hitherto collected supporting the notion of UPF3A being an NMD suppressor while UPF3B supports NMD, I decided to generate double mutant mice lacking both UPF3A and UPF3B to test if these mutations would cancel each other out and result in a rescue of function in the OE. As a proxy for an olfactory defect, I measured weight at weaning, just as I previously did for *Upf3a*$^{+/-}$ mice (figure 5A). I observed that *Upf3a*$^{+/-}$; *Upf3b*$^{+/-}$ and *Upf3a*$^{+/-}$; *Upf3*$^{-/*-}$ mice had a statistically significant decrease in body weight, but it was very modest at around 5% (figure 13A). While the decrease is modest, it shows improvement from the *Upf3b*$^{-/*}$ pups, which were ~25% smaller (figure 5A). My finding that loss of one copy of *Upf3a* partially rescues the defect caused by complete loss of *Upf3b* supports the hypothesis that these two paralogs functionally oppose each other.

As described above, qPCR analysis of OSN markers serves as a proxy of the relative quantities of olfactory cells at different stages of development. This

analysis revealed that double-mutant mice expressed HBC and mOSNs markers at very similar level as control mice; there was no statistically significant difference in their levels (figure 14C). This provided evidence that OSN defects caused by perturbation of either UPF3A or UPF3B alone were corrected when both UPF3A and UPF3B were perturbed.

I also used the RNA to check for changes in the magnitude of NMD, by examining the relative quantities of RNAs involved in UPR and TGF-β signaling that have been shown to be direct NMD targets. Compared to the *Upf3a*- and *Upf3b*-single mutants, the *Upf3a/Upf3b*-double mutant mice had NMD substrate levels reflecting a more normal level of NMD. While many of these NMD substrates had a significant down-regulation (~50%), this was not nearly as dramatic as in *Upf3a-cKO* mice, which showed 75-90% reduction in most of the targeted RNAs (figure 15C). When plotted together, it is easier to observe that loss of UPF3A results in significant down-regulation of NMD targets, while loss of UPF3B causes an increase in NMD substrates, but when both are mutated the levels of NMD are closer to the wild-type control (figure 15D).

I then wanted to test if the double mutant mice had functional recovery in mOSN regeneration. I treated the mice with methimazole to chemically ablate the mOSNs and measured the OE thickness. The double-mutant mice had an increased ability to regenerate neurons compared to single-mutant mice. Indeed, the double-mutant mice had OE thickness comparable to wild-type mice (figure 16). These data together showed that complete loss of UPF3B coupled with

haploinsufficiency of UPF3A cancel each other out, leading to rescue of many of the defects caused by loss or depletion of UPF3A or UPF3B alone.

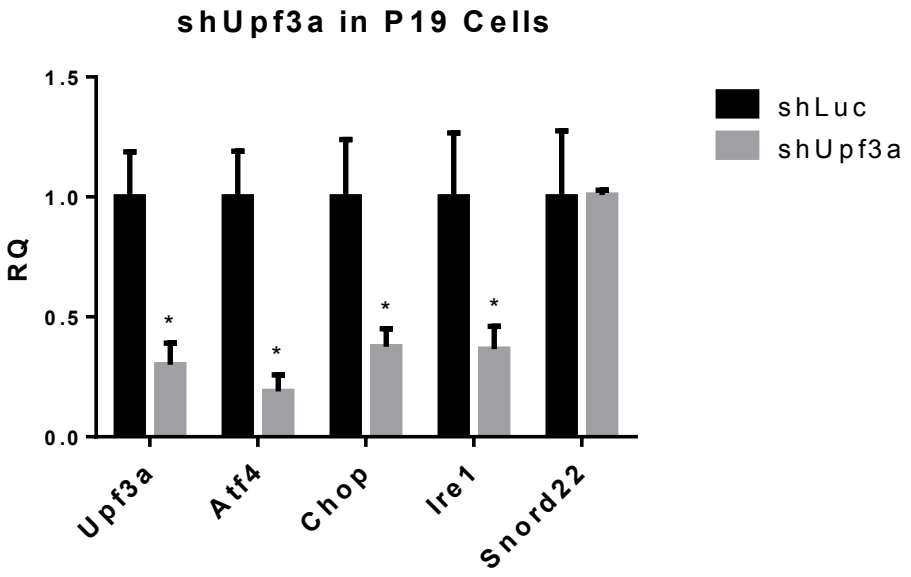

Figure 1: UPF3A is an NMD Inhibitor

Upf3a knockdown by *shUpf3a* transfected into P19 cells. *Upf3a* was knocked down by ~70%. Depletion of *Upf3a* leads to a decrease in the level of the NMD substrates shown. This is the opposite result expected from depletion of a *bona fide* NMD factor. Control samples were transfected with a luciferase reporter vector. The experiment was performed with three biological replicates and three technical replicates each. The results shown are from one biological replicate and three technical replicates. While results from most experiments were consistent, some NMD target mRNAs exhibited considerable fluctuation in levels in some experiments, based on my qPCR analysis. Significance ($P<0.05$) indicated by an asterisk.

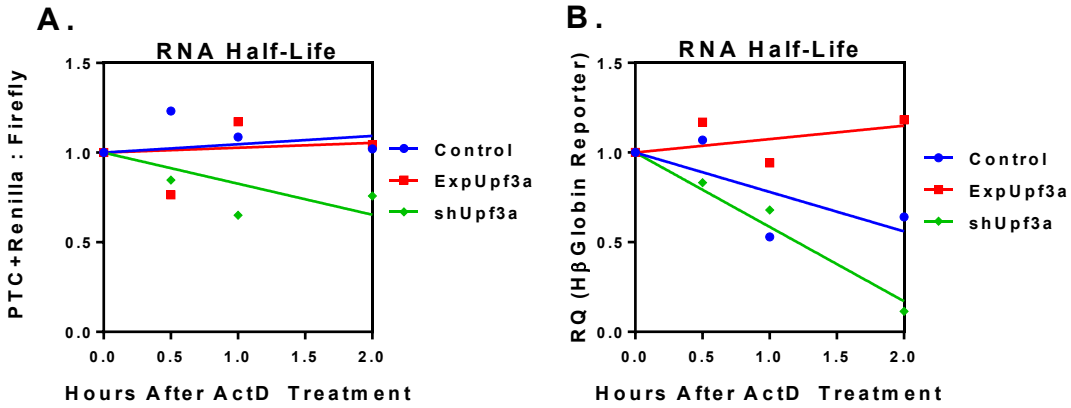

Figure 2: UPF3A Stabilizes NMD Substrate RNAs

A. RNA half-life experiment measuring RNA degradation. Performed by transfecting P19 cells with PTC-/PTC+ NMD construct cloned into renilla and firefly luciferase reporters. Samples were also given either *shUpf3a*, *ExpUpf3a*, or empty vector control. 24 hours post-transfection cells were treated with ActD, the RNA was collected, and analyzed via qPCR by taking ratio of firefly (PTC+) and renilla (PTC-) quantities and normalized to 0 hours for all samples. Knockdown of *Upf3a* results in destabilization of reporter RNA, and overexpression does not result in a significant change. Experiment was performed with two biological replicates and two technical replicates. Both replicates showed similar results.

B. RNA half-life analysis. Same procedure as B, but I measured *HBG* as endogenous control and measured the degradation of the firefly reporter. *Upf3a* knockdown results in greater RNA decay, while *Upf3a* overexpression leads to RNA stability.

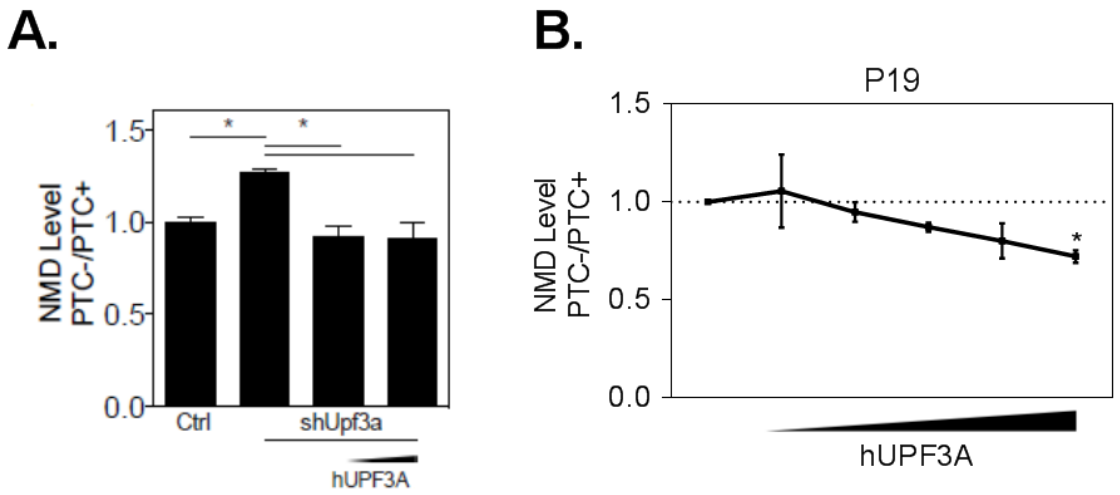

Figure 3: UPF3A's NMD Repressor Activity is Evolutionarily Conserved

A. Transfection of *hUpf3a*, *shUpf3a*, and PTC-/PTC+ NMD reporter into mouse P19 cells. Control sample was transfected with empty vector. Other samples were transfected with equal amounts of shUpf3a and increasing amounts of *hUpf3a*. Knockdown of *Upf3a* resulted in greater NMD activity. Overexpressing Upf3a resulted in a repressing NMD back to endogenous levels. All samples normalized to control. Two biological replicates and two technical replicates were performed; one by myself and the other by Eleen Shum. Results shown are from one biological replicate, both experiments showed similar results. Significance ($P<0.05$) indicated by an asterisk.
B. Transfection titration of *hUpf3a* and PTC-/PTC+ NMD reporter into P19 cells. Samples normalized to control transfected with empty vector. Serial dilution of plasmid of *hUpf3a* from 100ng to 6.25ng was performed to observe dosage response. Adding human form of *Upf3a* into mouse cells was able to repress NMD in a dose-respondent manner. Two biological replicates and two technical replicates were performed; one by myself and the other by Eleen Shum.. Results shown are from one biological replicate, both experiments showed similar results. Significance ($P<0.05$) indicated by an asterisk.

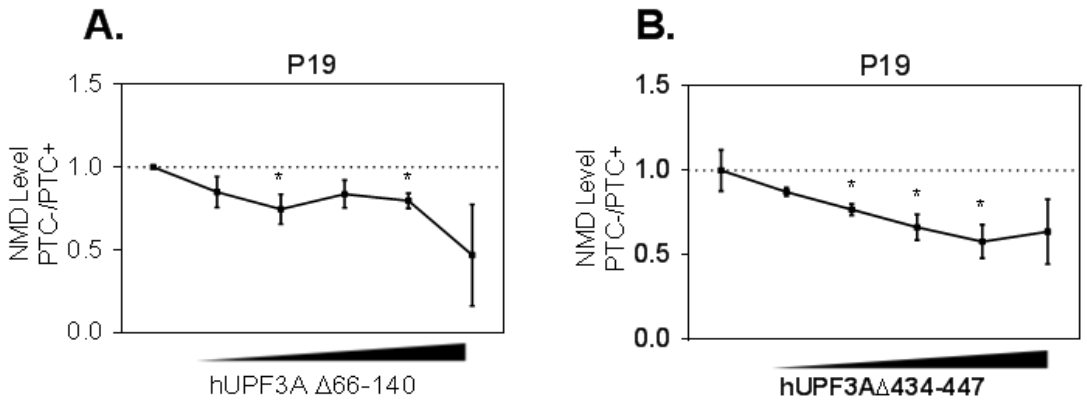

Figure 4: UPF3A's NMD Repressor Activity Requires Amino Acids Encoded by Exon 4

A. Titration transfection of P19 cells with PTC-/PTC+ NMD reporter and mutant hUPF3AΔ66-140, which abolishes UPF2 interactions. Serial dilution was of plasmid with mutant hUPF3A from 100ng to 6.25ng was performed to measure dosage response. This mutant form of UPF3A was sufficient to repress NMD activity. Two biological replicates and two technical replicates were performed; one by myself and the other by Eleen Shum.Results shown are from one biological replicate, both experiments showed similar results. Significance ($P<0.05$) indicated by an asterisk.

B. Titration transfection of P19 cells with PTC-/PTC+ NMD reporter and mutant hUPF3AΔ434-447, which abolishes Y14 interactions. Serial dilution was of plasmid with mutant hUPF3A from 100ng to 6.25ng was performed to measure dosage response. This UPF3A mutant was sufficient to repress NMD activity. Two biological replicates and three technical replicates were performed; two by myself and the other by Eleen Shum.. Results shown are from one biological replicate, two experiments showed similar results while one showed no change. Significance ($P<0.05$) indicated by an asterisk

C. Titration transfection of P19 cells with PTC-/PTC+ NMD reporter and hUPF3AΔE4. Serial dilution was of plasmid with mutant hUPF3A from 100ng to 6.25ng was performed to measure dosage response. This UPF3A mutant was did not have any effect on NMD activity. Three biological replicates and three technical replicates were performed; two by myself and the other by Eleen Shum.Results shown are from one biological replicate, all three showed similar results. Significance ($P<0.05$) indicated by an asterisk

D. Rescue of NMD performed by knocking down UPF3A and addition of one of the hUPF3A plasmids. P19 cells were transfected with shUpf3a, NMD reporter, and one of the forms of hUPF3A. All of the UPF3A mutants with the exception of the ΔE4 mutant were able to rescue NMD activity from the *Upf3a* shRNA. Three biological replicates and two technical replicates were performed; two by myself and the other by Eleen Shum. Results shown are from one biological replicate, two experiments showed similar results while one had a differedifferent effect. Significance ($P<0.05$) indicated by an asterisk.

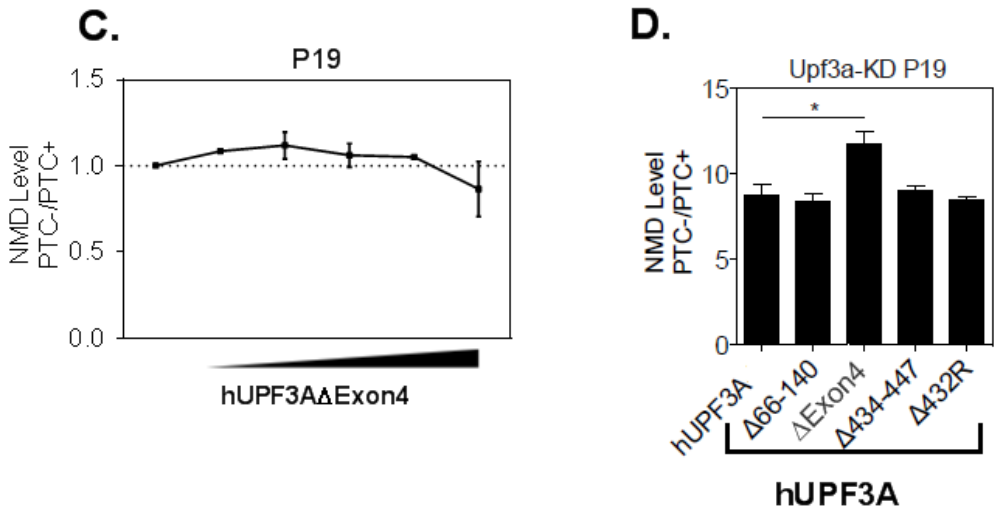

Figure 4. continued

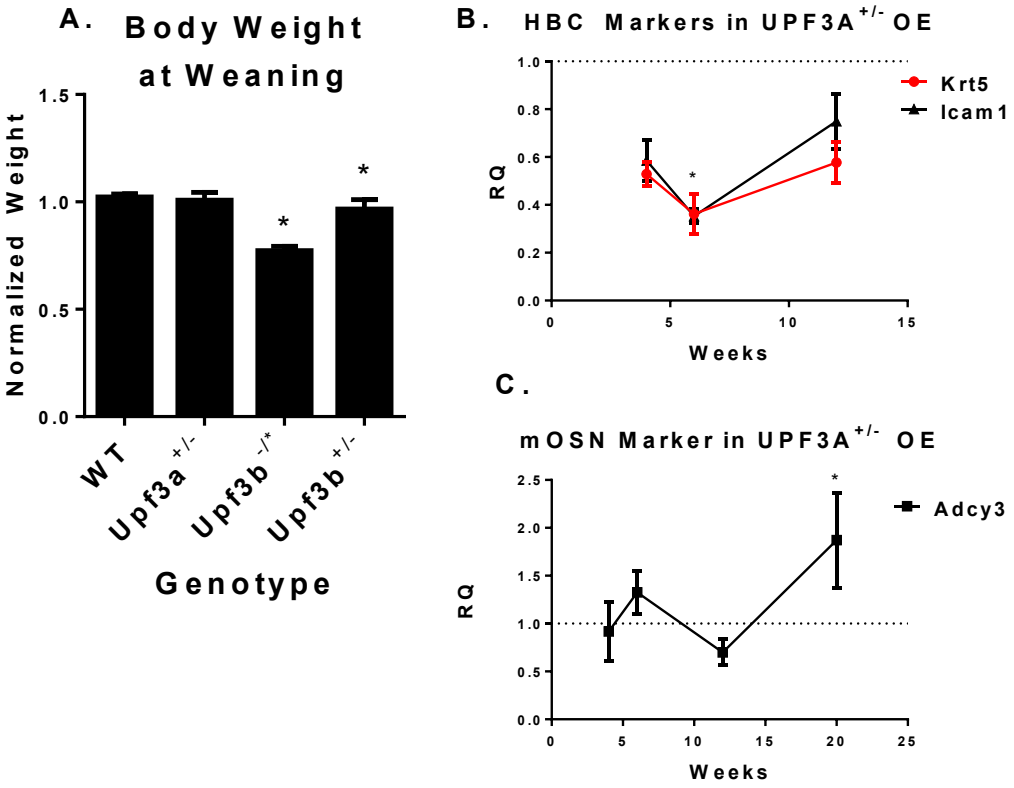

Figure 5: Olfactory Defects in *Upf3a*$^{+/-}$ Mice

A. Body weight of mice at time of weaning. At P21, mouse pups were weaned and weighed. After the genotypes had been determined, the mice were normalized to the wild-type littermates of the same gender. *Upf3b*$^{-/*}$ (*Upf3b*$^{-/Y}$ males and *Upf3b*$^{-/-}$ females) mice and *Upf3b*$^{-/+}$ female mice had significantly decreased body weight relative to control (WT) mice. *Upf3a*$^{+/-}$ mice weight was not significantly different than that of control mice. For numbers of mice: n=13 for WT, n=6 for *Upf3a*$^{+/-}$, n=5 for *Upf3b*$^{-/*}$, and n=6 for *Upf3b*$^{-/Y}$. Significance ($P<0.05$) indicated by an asterisk.

B. RNA levels of OE cell types were measured over time. *Krt5* and *Icam1* are two markers unique to HBCs. There is a reduction in HBC markers for all time points. Results shown are from one biological replicate for each time point and three technical replicates. At for weeks WT n=1 and Upf3a$^{+/-}$ n=2. At six weeks WT n=2 and *Upf3a*$^{+/-}$ n=4. At 12 weeks WT n=2 and *Upf3a*$^{+/-}$ n=2. At 20 weeks WT n=2 and *Upf3a*$^{+/-}$ n=2. Significance ($P<0.05$) indicated by an asterisk.

C. RNA levels of OE cell types were measured over time. *Adcy3* is a marker of mOSNs. The mOSN marker fluctuates until it seems to be up-regulated, indicating more mOSNs in the *UPF3A*$^{+/-}$ relative to wild type. Same mice were used as in panel b. Significance ($P<0.05$) indicated by an asterisk.

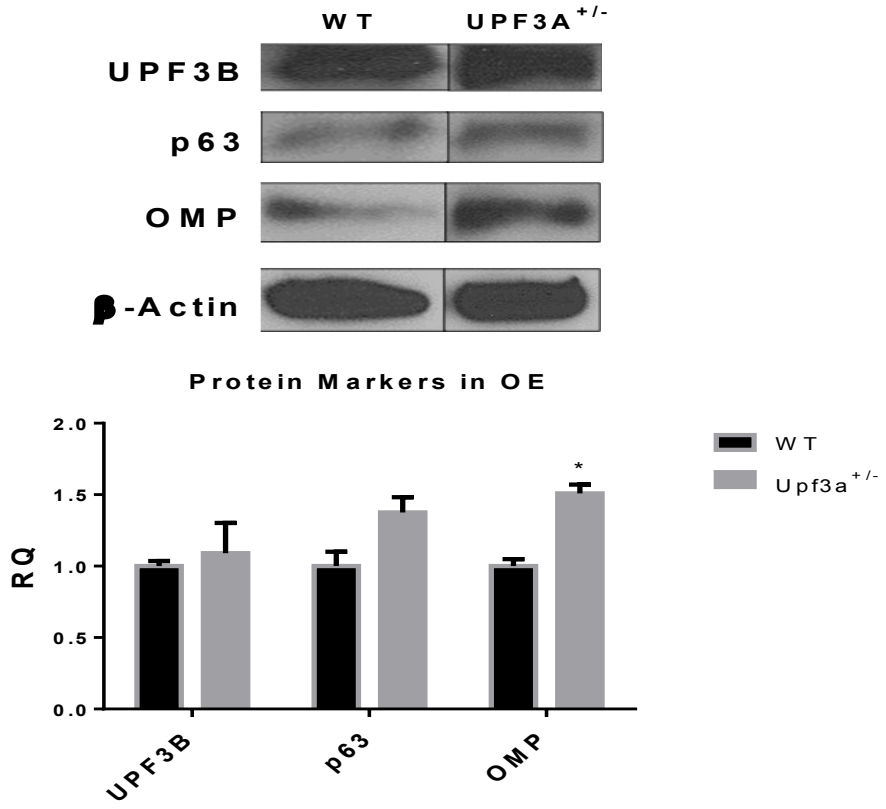

Figure 6: *Upf3a*$^{+/-}$ OE has Elevated Levels of OMP Protein Expression

A. Western blot of proteins form mouse OE. Adult mice were sacrificed, the OE was extracted, and the proteins were purified. This western blot shows that in response to UPF3A haploinsufficiency there is little to no change in the UPF3B or p63 protein expression, but a significant increase in OMP. Relative quantities were measured using imageJ software©. Two wild-type and two *Upf3a*$^{+/-}$ mice were used. Charts show normalization of relative protein quantities. Experiment was performed three times, but only once successfully. Significance ($P<0.05$) indicated by an asterisk.

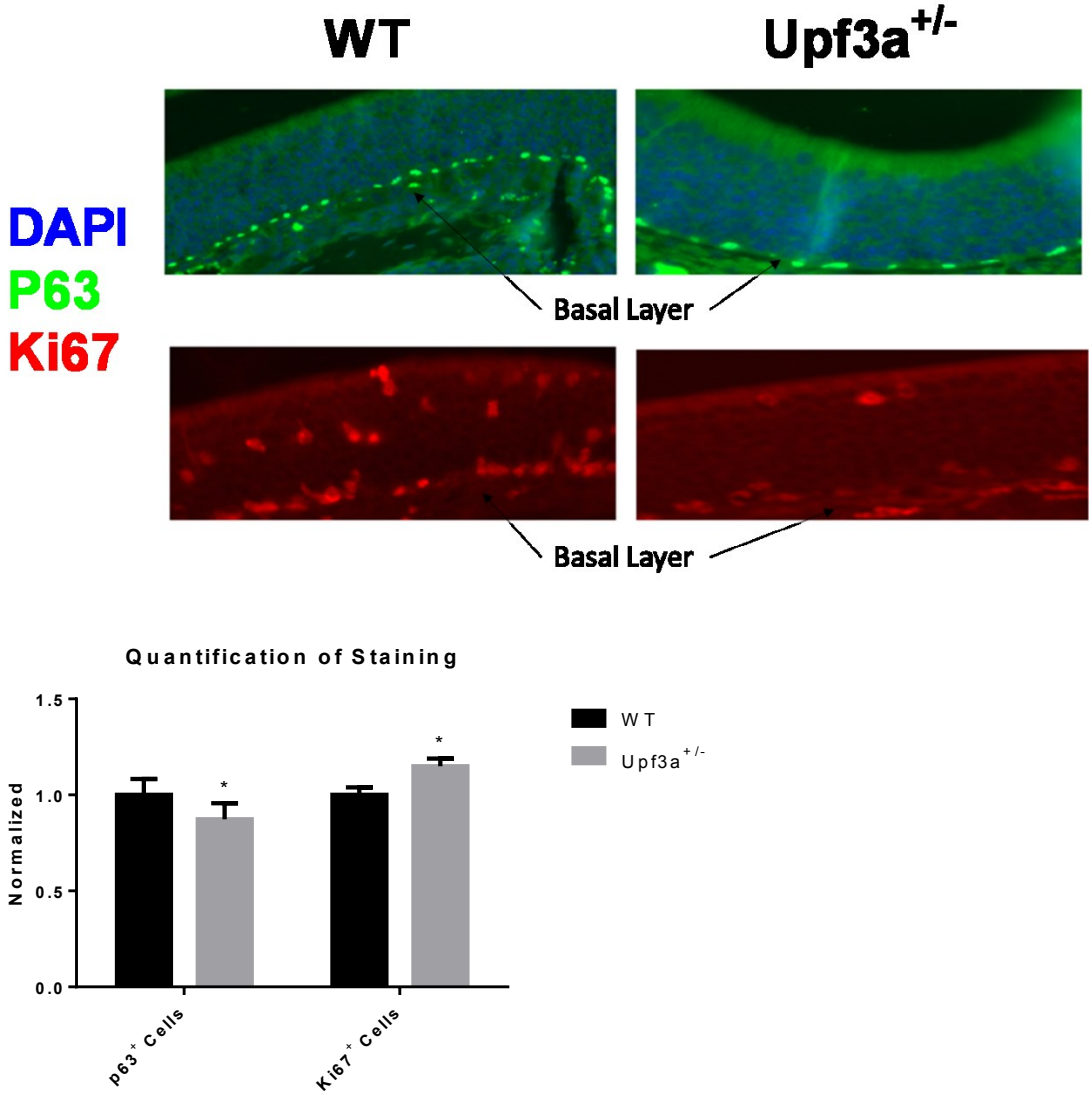

Figure 7: *Upf3a*$^{+/-}$ OE has Reduced Numbers of HBCs and Increased Numbers of Ki67+ Cells

A. Fluorescent images of OE taken from a six week old *Upf3a*$^{+/-}$ mouse. p63 is a marker for HBCs. There is a slight, but significant reduction in the amount of p63+ cells in the *Upf3a*$^{+/-}$ relative to wild type. Ki67 is a marker for proliferation. There was an increase in proliferation, particularly in the middle layers of the OE in the *Upf3a*$^{+/-}$ relative to the wild type. Cells were counted for quantification and represented by the accompanying charts. Experiment was performed once. Two wild-type and two *Upf3a*$^{+/-}$ mice were used. Significance ($P<0.05$) indicated by an asterisk.

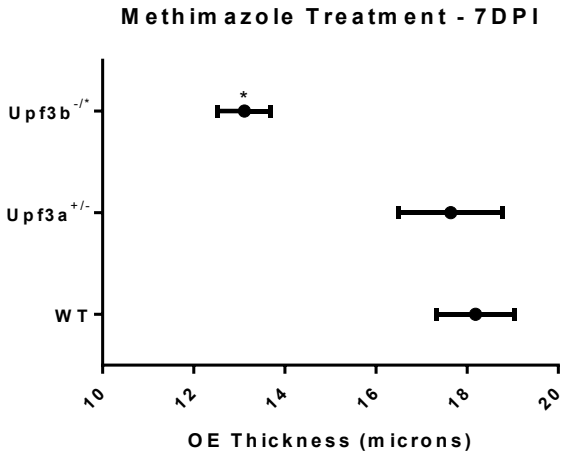

Figure 8: *Upf3a*$^{+/-}$ OE Thickness is Not Significantly Different than that of Control OE

A. Measurement of OE thickness following chemical ablation by methimazole injection. Mice were administered with methimazole via intraperitoneal injection and allowed one week to recover. Following one week the mice were sacrificed. Measurements of the OE thickness were taken. The wild type and *Upf3a*$^{+/-}$ mice show no significant different while the *Upf3b*$^{-/*}$ mice show a defect with OE regeneration 25% less compared to the wild type. Experiment was performed twice with similar results. One mouse from each genotype was used. Significance ($P<0.05$) indicated by an asterisk.

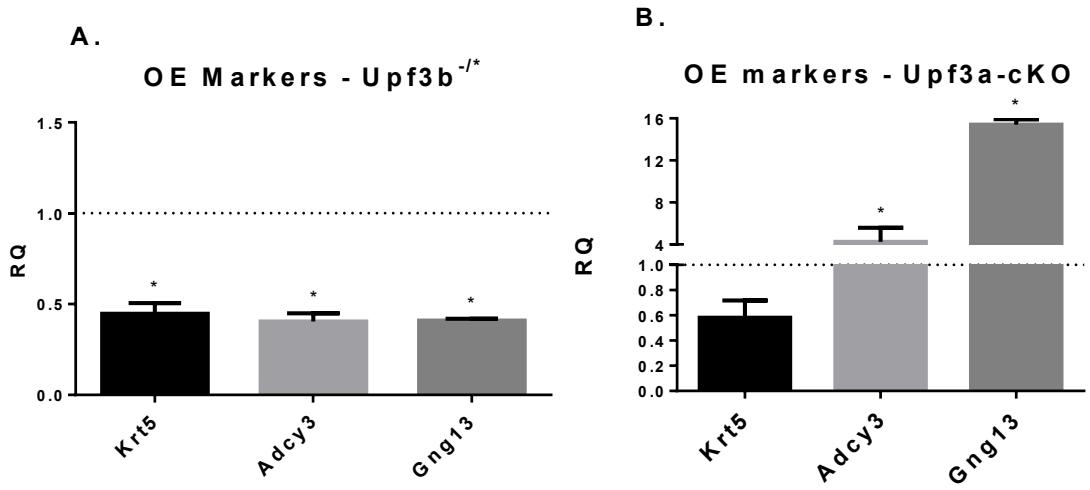

Figure 9: *Upf3a*-cKO Mice have Dramatically Increased Levels of mOSN Markers

A. RNA levels of HBC and mOSN markers were quantified in *Upf3b*$^{-/*}$ mice using qPCR. *Krt5* was used as a marker for HBC cells, while *Adcy3* and *Gng13* were used as markers for mOSNs. There is a reduction of both HBC and mOSN markers which agrees with pervious findings in the Upf3b$^{-/*}$ mice. Results shown are from one biological replicate and three technical replicates. Number of mice used: n= 2 wild-type and n=4 *Upf3b*$^{-/*}$ mice used. Significance ($P<0.05$) indicated by an asterisk.
B. RNA levels of HBC and mOSN markers were quantified in *Upf3a-cKO* mice using qPCR. The mice were given a tamoxifen diet for two weeks to induce cre expression. *Krt5* was used as a marker for HBC cells, while *Adcy3* and *Gng13* were used as markers for mOSNs. There was a reduction of *Krt5* indicating fewer HBCs, but this difference was not significant. The mOSNs markers were both highly up-regulated to a significant level. This supports the previous data from the *Upf3a*$^{+/-}$ mice that had reduced HBC markers and increased mOSNs. Results are shown from one biological replicate and three technical replicates. Number of mice used: n=4 wild-type and n=2 *Upf3a-cKO* mice. Significance ($P<0.05$) indicated by an asterisk.

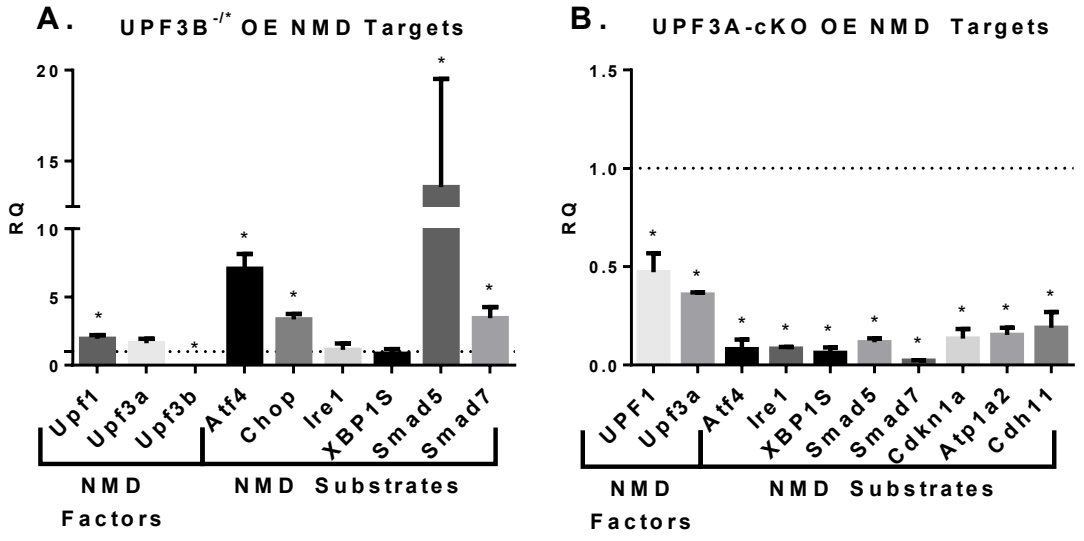

Figure 10: Evidence that *Upf3a*-cKO Mice have Hyper NMD

A. Relative quantities of different NMD substrates were measured in *Upf3b*$^{-/*}$ mice. Many different putative NMD targets were tested, and most saw significant up-regulation. There was a particularly significant increase in *Smad5* and *Smad7* mRNA, which encode proteins involved in TGF-β signaling. There was also significant up-regulation of many UPR genes, but not *XBP1S* (which is not an NMD target but a marker of cellular stress) indicating that the cells were not subject to ER stress. Number of mice used: n= 2 wildtype and n=4 *Upf3b*$^{-/*}$ mice used. Significance ($P<0.05$) indicated by an asterisk.
B. Relative quantities of different NMD substrates were measured in *Upf3a-cKO* mice. The mice were given a tamoxifen diet for two weeks to induce cre expression. All of the targets tested had a significant down-regulation. *UPF1* had the most modest decrease of only around 50%, which indicates that NMD was very strong in down-regulating its substrates, including its own factors. Both genes involved in UPR and TGF-β were significantly down-regulated indicating very little cellular stress and very little anti-proliferative genes. This fits with the other data that indicate more differentiation and proliferation in the UPF3A deficient mice. Number of mice used: n=4 wild-type and n=2 *Upf3a-cKO* mice. Significance ($P<0.05$) indicated by an asterisk.

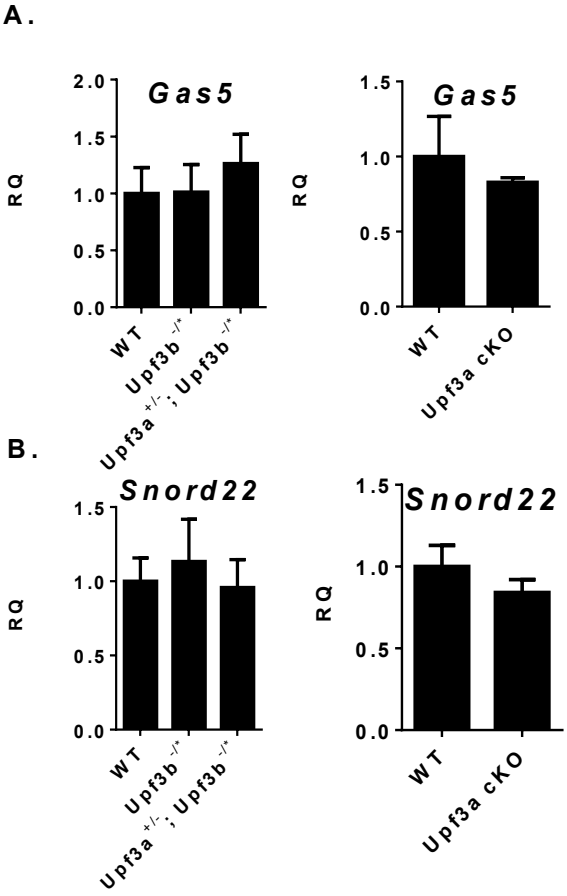

Figure 11: Evidence that Long Non-Coding RNAs are Immune to UPF3A Regulation

A. Analysis of *Gas5* long non-coding RNA (a known NMD target transcript) in *Upf3b*$^{-/*}$*, Upf3a-cKO*, and double mutant mice. The *Upf3acKO* mice were given a tamoxifen diet for two weeks to induce active Cre. In all of the samples there was no significant up or down-regulation of the substrate. This suggests that *Gas5* is independent of both UPF3A and UPF3B in the OE. Results from single biological replicates and three technical replicates. Number of mice used: n=2 wild-type, n=4 Upf3b$^{-/*}$, and n=2 *Upf3a*$^{+/-}$; *Upf3b*$^{-/*}$. Also used n=4 wild-type littermates compared to n=2 Upf3a cKO mice. Significance (P<0.05) indicated by an asterisk.
B. Same procedure as panel A, but with the *Snord22* long non-coding RNA, a known NMD target transcript. Significance (P<0.05) indicated by an asterisk.

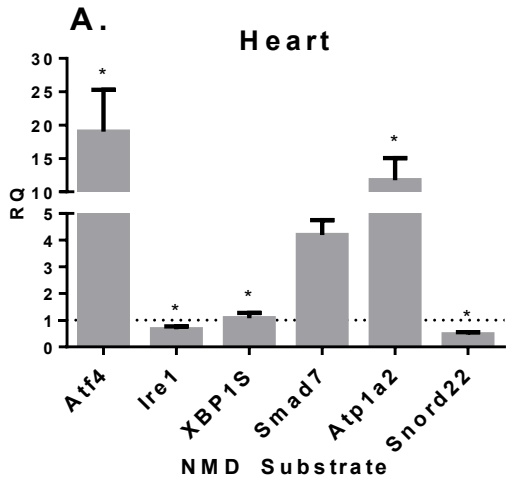

Figure 12: Evidence that UPF3A's Effects on NMD are Tissue Specific

A. Quantification of NMD substrates in heart tissue from *Upf3a*$^{+/-}$ mice. The heart displays a very different expression pattern, and only a moderate level of UPF3A expression. While loss of UPF3A in P19 cells and the OE has thus far shown down-regulation of nearly every NMD substrate, the heart shows that some targets are up while others are down-regulated. Results are from one biological replicate and three technical replicates. Used n=1 WT mice and n=2 *Upf3a*$^{+/-}$ mice. Significance ($P<0.05$) indicated by an asterisk.
B. Quantification of NMD substrates in the brain from *Upf3a*$^{+/-}$ mice. The brain, like the heart, expresses a moderate level of UPF3A. While composed of neurons, like the OE, there are many different cell types in the brain, making it thus more difficult to predict NMD activity. Used n=1 WT mice and n=2 *Upf3a*$^{+/-}$ mice Significance ($P<0.05$) indicated by an asterisk.
C. Quantification of NMD substrates in the spleen from *Upf3a*$^{+/-}$ mice. The spleen has been shown to have little UPF3A. The spleen shows a consistent down-regulation of genes involved in the UPR, as seen in the OE; also, *Snord22* has a statistically insignificant change. Used n=1 WT mice and n=2 *Upf3a*$^{+/-}$ mice Significance ($P<0.05$) indicated by an asterisk.

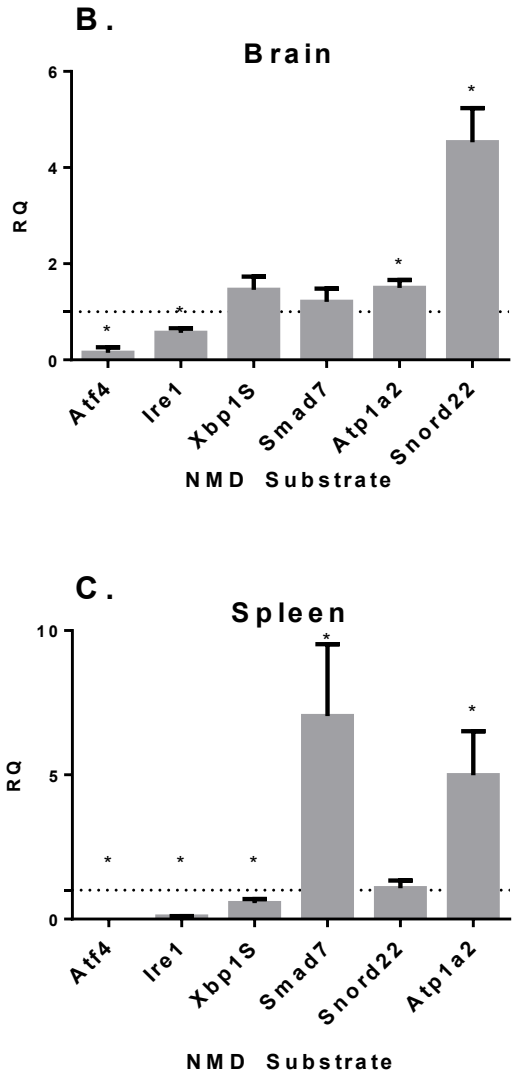

Figure 12. continued

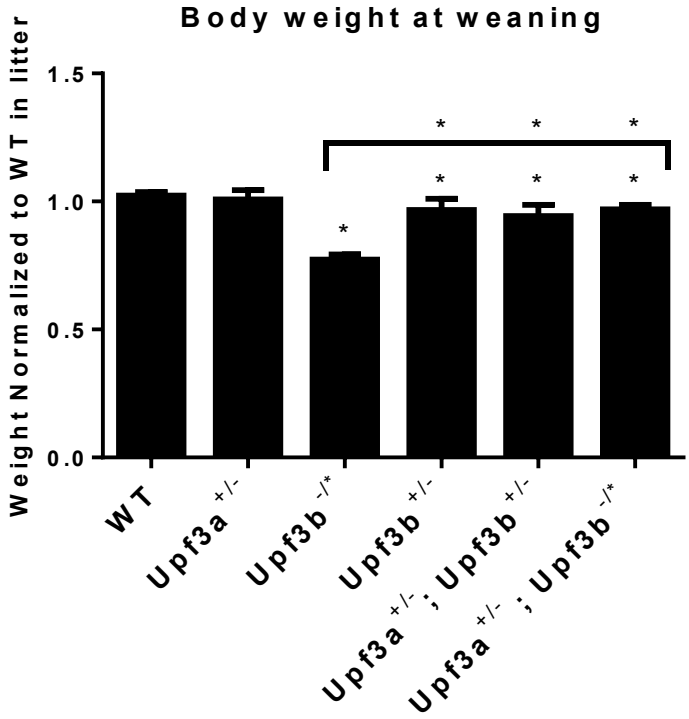

Figure 13: Loss of One Copy of *Upf3a* Partially Rescues the Weaning Weight Defect Caused by Complete Loss of *Upf3b*

A. Body weight of mice at the time of weaning. At p21 the mice are weaned and weighed. The *Upf3a*$^{+/-}$; *Upf3b*$^{-/*}$ mice, male and female, show a significant decrease in body weight. While the decrease in body weight is statistically, significant the difference is only around 5%. This is an increase from the 25% reduction of the *Upf3b*$^{-/*}$ mice. For numbers of mice: n=13 for WT, n=6 for *Upf3a*$^{+/-}$, n=5 for *Upf3b*$^{-/*}$, n=6 for *Upf3b*$^{-/+}$, n=5 *Upf3a*$^{+/-}$; *Upf3b*$^{+/-}$, and n=4 *Upf3a*$^{+/-}$; *Upf3b*$^{-/**}$. Significance ($P<0.05$) indicated by an asterisk.

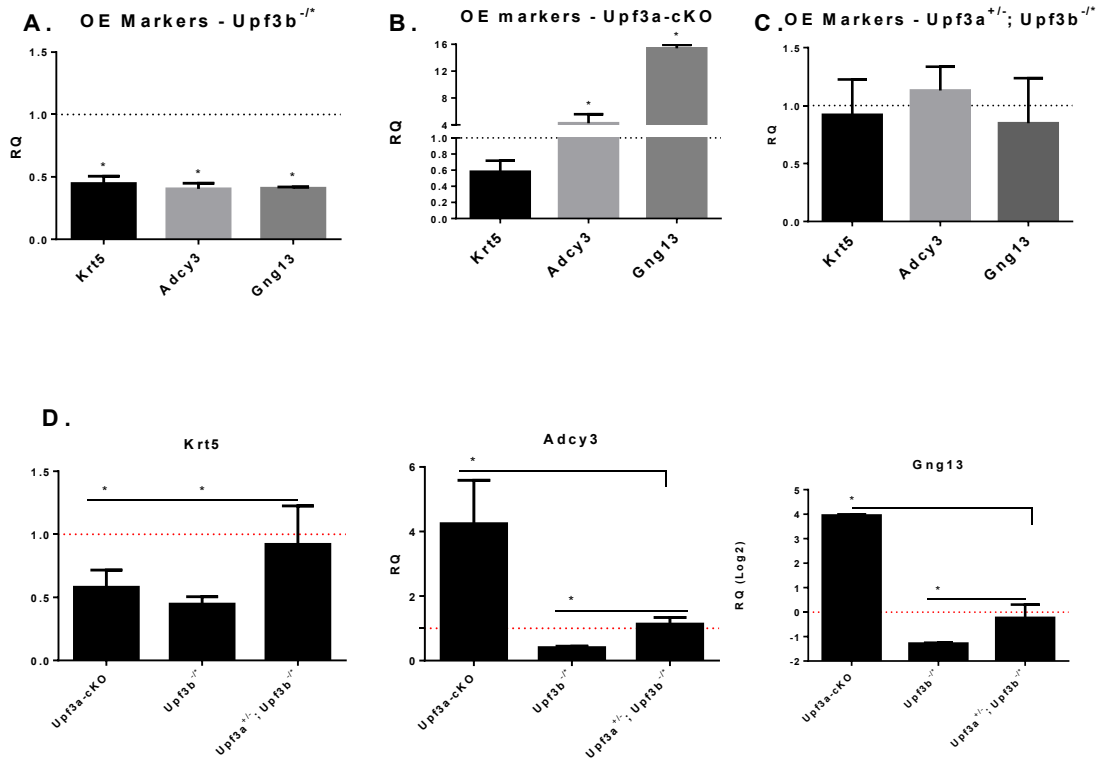

Figure 14: Partial Loss of *Upf3a* in OSNs Largely Rescues the HBCs and mOSN Marker Defects Caused by Loss of *Upf3b*

Quantification of OE markers from double mutant mouse OE. Using *Krt5* as a marker to measure the HBC population there is an insignificant difference between the double mutant mice and the wild type. *Adcy3* and *Gng13* were both used as markers to measure mOSN populations. Both makers showed an insignificant difference relative to wild type. This suggests that loss of UPF3A can help rescue the effects resulting from UPF3B loss. Results shown are from different, single biological replicates each with three technical replicates. Number of mice used: n= 2 wild-type, n=4 *Upf3b*$^{-/*}$, and n=2 double mutant* mice used. Also used n=4 wild-type littermates compared to n=2 *Upf3a-cKO* mice. Significance (P<0.05) indicated by an asterisk.

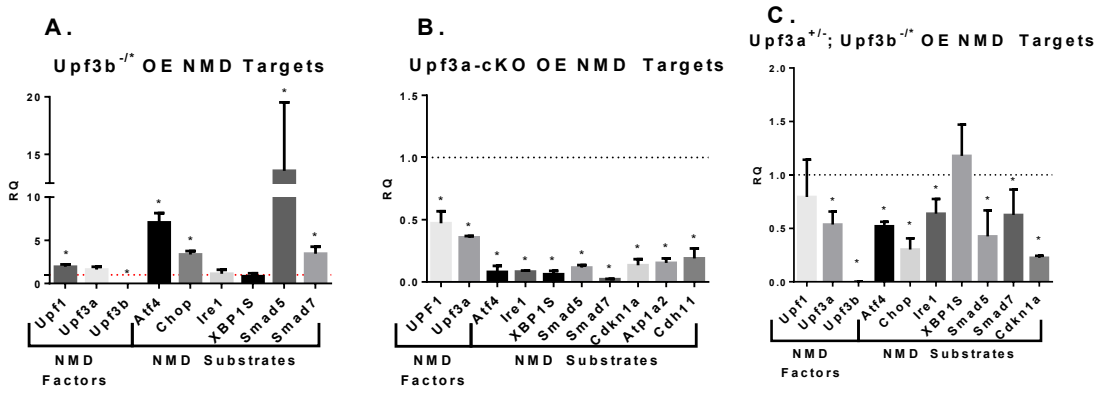

Figure 15: Partial Loss of *Upf3a* in OSNs Partially Rescues the Defects in NMD Caused by Loss of *Upf3b*

A. Quantification of NMD targets in the *Upf3b*$^{-/*}$ OE. Many different putative NMD targets were tested, and most saw significant up-regulation. Results shown are from different, single biological replicates each with three technical replicates. Number of mice used: n= 2 wild-type and n=4 *Upf3b*$^{-/*}$. Significance (P<0.05) indicated by an asterisk.
B. Relative quantities of different NMD substrates were measured in *Upf3a*-cKO mice. The mice were given a tamoxifen diet for two weeks to induce cre expression. All of the targets tested had a significant down-regulation. Results shown are from different, single biological replicates each with three technical replicates. Number of mice used: n=4 wildtype and n=2 *Upf3a*-cKO mice. Significance (P<0.05) indicated by an asterisk.
C. Quantification of NMD targets in the double mutant OE. While many of the NMD targets are significantly downregulated, it is a reversal of the effect seen in the *Upf3b*$^{-/*}$ which resulted in significant up-regulation of NMD substrates. Results shown are from different, single biological replicates each with three technical replicates. . Number of mice used: n= 2 wild-type and n=2 double mutant mice used. Significance (P<0.05) indicated by an asterisk.
D. Data from panels A, B, and C plotted together on a logarithmic scale. NMD targets from the *Upf3a*-cKO OE are below 0, the NMD targets from the *Upf3b*$^{-/*}$ OE are above 0, and the NMD targets from the double mutant OE are closer to 0, suggesting a partial rescue in NMD activity.

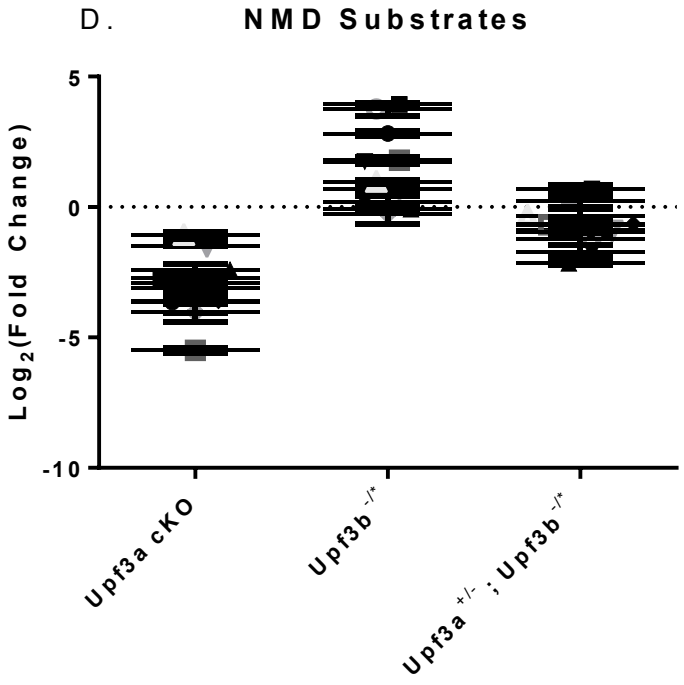

Figure 15. continued

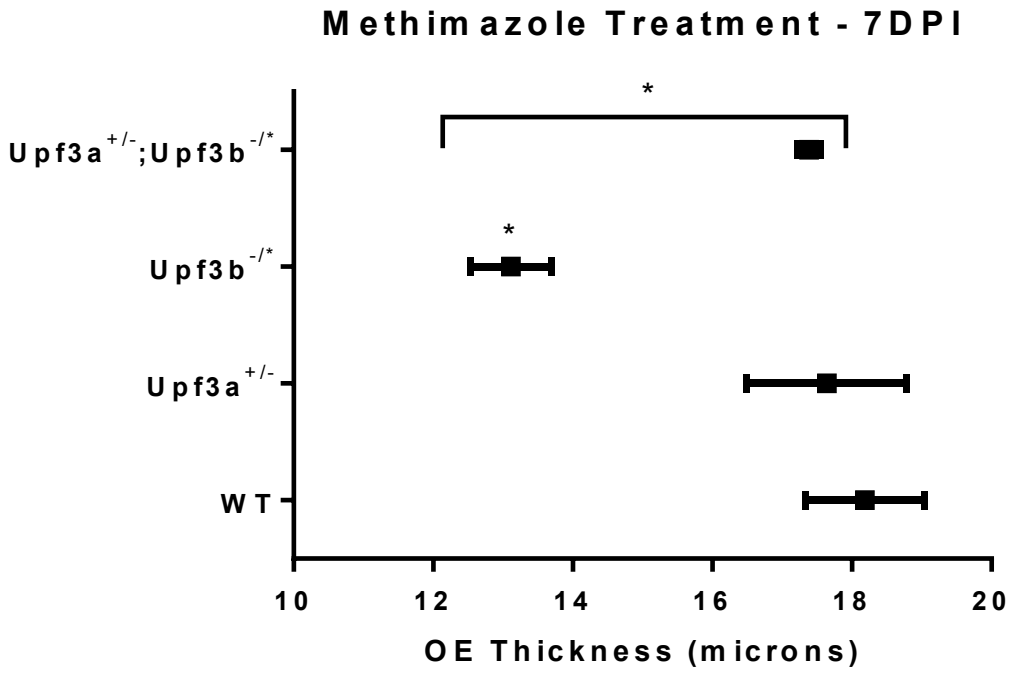

Figure 16: Partial Loss of *Upf3a* in OSNs Largely Rescues the OE Defect Caused by Loss of *Upf3b*

Measurement of OE thickness following chemical ablation by methimazole injection. Mice were administered with methimazole via intraperitoneal injection and allowed one week to recover. Following one week the mice were sacrificed. Measurements of the OE thickness were taken. The wild type, *Upf3a*$^{+/-}$, and *Upf3a*$^{+/-}$; *Upf3b* $^{-/*}$ mice show no significant change. The Upf3b$^{-/*}$ mice show a regenerative defect with 25% thinner OE compared to the wild type. The rescued effect seen between theUpf3b$^{-/*}$ and Upf3a$^{+/-}$;Upf3b$^{-/*}$ mice supports other data that loss of UPF3A can compensate for loss of UPF3B. Experiment was performed twice with similar results. Results shown are from one biological replicate. Number of mice used: n=1 WT, n=1 *Upf3a*$^{+/-}$, n=1 *Upf3b*$^{-/*}$, and n=2 *Upf3a*$^{+/-}$;*Upf3b* $^{-/*}$. Significance ($P<0.05$) indicated by an asterisk.

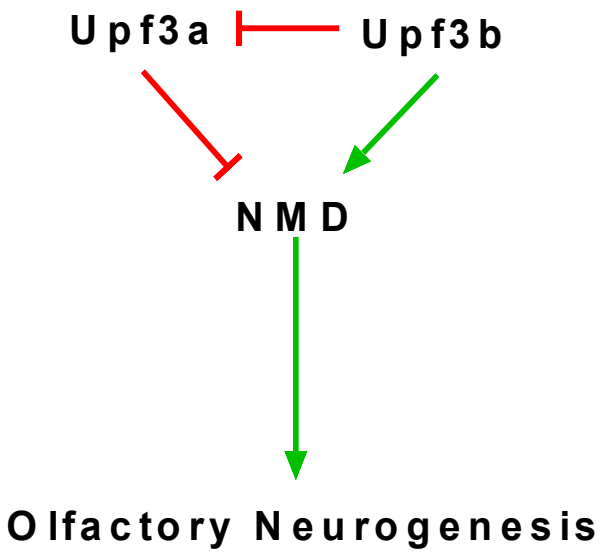

Figure 17: Model

Published data, coupled with my data reported herein, strongly suggest that UPF3A is an NMD repressor, while UPF3B is an NMD activator. When the magnitude of NMD is stronger than normal (de-repressed in *Upf3a*$^{+/-}$ and *Upf3a-cKO* mice), there is an increase in olfactory neurogenesis. When NMD is inhibited (in *Upf3b*-null mice), there is less OSN proliferation and fewer mOSNs. When NMD magnitude is restored to nearly normal by depletion of both UPF3A and UPF3B in the double mutantmice, a relatively normal olfactory phenotype is restored.

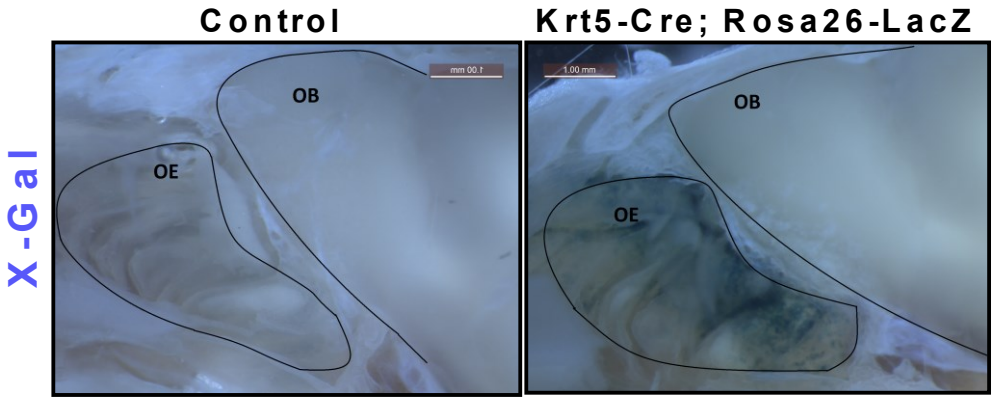

Supplemental Figure 1: LacZ Reporter Indicating *Krt5* Promoter Driven Expression of CRE-Recombinase is Specific to the OE

The mice were given a tamoxifen diet for two weeks to induce cre expression. After two weeks the mice were administered with methimazole via intraperitoneal injection. One week following injection, the OE was extracted and fixed. X-gal staining shows where there was LacZ expression as driven by the *Krt5* promoter. The blue in the reporter mice is specific to the OE and does not appear in other parts of the brain or other tissues, indicating specificity of the *Krt5*-Cre.

III:

Discussion

UPF3A is a NMD Repressor

The UPF3A and UPF3B paralog pair are evolutionarily ancient, having arisen ~500 million years ago at the dawn of the vertebrate lineage. It has been assumed that these two gene paralogs act in a redundant fashion to promote NMD (Lykke-Andersen *et al.* 2000, Chan *et al. 2009*). My discovery that UPF3A generally does not promote NMD, but rather acts as an NMD inhibitor, suggests a new view of the functional relationship of these two paralogs. By acting in opposition, I suggest that these factors control the magnitude of NMD in a tissue specific and developmentally regulated manner for the purpose of controlling development. In other words, the UPF3A/UPF3B paralog pair was maintained during evolution for the purpose of controlling appropriate levels of RNA decay depending on different developmental or other cues.

The finding that UPF3A is primarily a NMD repressor has implications for understanding the branches of NMD. Previous evidence suggested that UPF3A's paralog, UPF3B, is required for a specific branch of NMD (Chan *et al.* 2007) but it has not been clear why only some NMD substrate mRNAs depend on UPF3B for their decay. One possibility is that UPF3B is a "branch specific" factor not because it is an essential NMD factor for some mRNAs, but rather because it is an NMD enhancer that only promotes the decay of a subset of mRNAs. These mRNAs might be those in which UPF3B rate limiting; for example, those in which UPF3B is required to form a bridge between UPF1 and the EJC in order to generate a RNA decay-promoting complex. UPF3A could act in this scenario by sequestering

essential factors from UPF3B or other components of the NMD machinery. Thus, according to this model, the UPF3A/UPF3B ratio would dictate whether a given mRNA was degraded by NMD and by how much. This predicts that the mRNAs that “depend” on UPF3B for their decay would differ in different cell types, depending on how much UPF3A they express. Future studies should be devoted to addressing this model.

I obtained several lines of evidence that the NMD repressive ability of UPF3A is conserved between mice and humans. I also obtained evidence that the portion of the UPF3A protein that confers its ability to repress NMD is encoded in the fourth exon. Why the 32 amino acids (141 to 172) encoded by exon 4 are required for NMD repression remains to be determined. Interestingly, exon 4 encodes part of the UPF3A domain used to interact with UPF2 (Onishi *et al.* 2003, Kunz *et al.* 2006, Leung *et al.* 2007). Indeed, X-ray crystallographic data from the analogous region of UPF3B shows that there are critical UPF2-direct binding residues within this region (Kadlec *et al.* 2004). This leads to the following model explaining how UPF3A represses NMD – UPF3A acts as an NMD decoy in order to sequester UPF2 from the rest of the NMD machinery in order to preclude RNA decay. Also consistent with this “sequestration model” is recent evidence from my laboratory indicating that depletion of UPF3A increases interactions between UPF1 and the EJC (Eleen Shum, unpublished data). The evidence against this model is my finding that the UPF3A mutant lacking residues 66-140, which includes amino acids known to interact with UPF2 (Kunz *et al.* 2006), is still capable of inhibiting NMD. This could be explained if it is shown that certain the amino acids

encoded by exon 4 are more important for UPF2 interaction than are amino acids 66-140. Another possibility is that the problem may not be a lack of binding, but perhaps the binding is so tight that the NMD machinery is immobilized on the RNA target and thus precluded from promoting decay. It is equally possible that a trans-acting, unknown, factor is involved that interacts with the amino acids encoded by exon 4. Mass spectroscopy analysis coupled with co-immunoprecipitation analyses could be used to identify such a factor.

While the NMD reporter I used provides one means of determining the effect on UPF3A on the magnitude of NMD, the approach falls shorts of conclusively showing the strength of NMD in all circumstances, particularly with regard to different NMD branches and NMD-inducing features in mRNA. Another potential approach to measure NMD strength is to perform a western blot and probe for phosphorylated UPF1, as UPF1 phosphorylation has been shown to be critical for NMD (Sweingruber *et al.* 2013). This might also show whether or not there is a change in a critical step of NMD required for RNA decay.

UPF3A's Role in *In Vivo* Development

Comparative analysis of *Upf3a*- and *Upf3b*-mutant mice provided several lines of evidence that UPF3A has functions that differ from UPF3B. First, complete loss of UPF3A is embryonic lethal, whereas loss of UPF3B is not (Huang *et al.*; Shum *et al.* manuscripts in preparation). Second, I found that *Upf3a*$^{+/-}$ mice do not exhibit the same olfactory related body weight deficiency seen in the *Upf3b*$^{-/*}$ mice. Third,

UPF3A-deficient (*Upf3a*$^{+/-}$ and *Upf3a-cKO*) mice show significant increases in mOSN markers, whereas UPF3B-deficient (*Upf3b*$^{-/*}$) mice have a decrease in such markers. Fourth, the relative amounts of NMD substrates is increased in *Upf3b*$^{-/*}$ mice, indicative of weakened NMD, as opposed to the *Upf3a-cKO*, which had down-regulated levels of most substrates, indicative of strong NMD. Finally, I found that *Upf3a*$^{+/-}$ mice did not have gross neuro-regenerative defects (as measured by OE thickness), whereas *Upf3b*$^{-/*}$ mice did.

My data showed that the UPF3A deficiency (either in heterozygous or conditional KO mice) caused altered expression of both HBC and mOSN markers. Given this, it was surprising that UPF3A-deficient mice did not have a defect in olfaction, at least as measured by weaning body weight. However, I only examined *Upf3a*-heterozygous mice, not *Upf3a*-cKO mice, so it remains to be determined whether complete loss of UPF3A impairs olfaction.

My finding that *Upf3a*-null mice have fewer HBCs and more mOSNs supports the notion that UPF3A is crucial for generating or receiving signals telling OSN-lineage cells to proliferate and/or differentiate. In further support of this, I observed that *Upf3a*$^{+/-}$ mice also had an abnormally high number of cells expressing proliferation marker Ki67. This high apparent rate of proliferation, coupled with the low level of HBC markers, may indicate that *Upf3a*-cKO mice have a defect in HBC self-renewal such that they have a tendency to differentiate into highly proliferative GBCs at the expense of HBC self-renewal. If so, this predicts that as they age, these *Upf3a*-cKO mice will develop overt olfactory

defects because of “stem cell exhaustion.” In addition to examining aged mice, an experiment to test this would be to provide a series of methimazole injections to serially deplete the OE of OSNs and thus tax the HBCs more quickly than would normally occur. As a consequence of repeated injuries the HBCs will be lost in a shorter amount of time as they are forced to divide more frequently. This would allow a stem cell defect in UPF3A-deficient mice to be evident more quickly than in non-treated mice. The reduction in HBCs could lead to their depletion over time, and this could be exacerbated in response to damage and injury.

Long Non-coding RNAs and UPF3 Proteins

I identified two NMD substrates whose levels were largely unaffected by loss of either UPF3A or UPF3B in the OE. This serves as additional evidence of branching in the NMD pathway. An additional point of interest is that both of these “UPF3 immune” NMD substrates are long non-coding RNAs. What makes long non-coding RNAs unique within this context is an interesting point to explore and may help elucidate the role of the UPF3 proteins in NMD, as well as NMD’s role as a surveillance pathway. Since long non-coding RNAs do not encode proteins of significant length, an issue that comes up is whether they are translated. This is important since NMD depends on translation in order for a PTC to be detected; mRNAs that are not translation are immune to NMD (Carter *et al.* 1996). While long non-coding RNAs do not encode proteins, many of them are translated, as shown by ribosome profiling (ref from NT Ingolia). For example, the NMD substrate, *Gas5* RNA, is a translated RNA that is a template for 10 snoRNAs

embedded in the introns (Smith et al. 1998). The exons appear to be non-functional and once the RNA is spliced the transcript has essentially served its purpose. NMD and other pathways could be used to degrade this transcript and within the context of the OE, the UPF3 proteins are of no particular significance. Further studies will have to elucidate the specifics of how this and other lnc-RNAs are degraded.

Interestingly, I found that the non-coding NMD substrate, *Snord22* mRNA, was differentially affected by loss of UPF3A in different tissues and cell types. While *Snord22* mRNA levels were not significantly affected by loss or depletion of UPF3A in OE, spleen, and in P19 cells, its levels were down-regulated in the heart and up-regulated in the brain of *Upf3a*-heterozygous mice. Whether this is the result of direct effects of UPF3A on NMD or indirect effects is not known. One explanation for why UPF3A deficiency does not lead to a change in *Snord22* mRNA levels within the OE and spleen is that it is so imperative this transcript be degraded for the proper function of these organs that other mechanisms compensate for inefficient or inhibited NMD. Together, these results reiterate the complex nature of the tissue and context specificity of NMD and all of the factors that play a role in its regulation.

UPF3A/UPF3B-Double Mutant Mice Have Less Severe Defects than Single-Mutant Mice

If indeed UPF3A is a NMD repressor and UPF3B is a NMD activating factor, this predicts that disruption of both might partially rescue defects caused by loss of only

one of these factors. I obtained several lines of evidence for this. First, I found that the weaning body weights of both double-mutant (*Upf3a*$^{+/-}$;*Upf3b*$^{+/-}$ and *Upf3a*$^{+/-}$;*Upf3b*$^{-/*}$) mice were significantly higher than that of single-mutant (*Upf3a*$^{+/+}$;*Upf3b*$^{*/-}$) mice. While the weights of the double-mutant mice were statistically lower than control mice (~5% reduction), the difference was very modest. This suggests (but does not prove) that loss of one copy of the *Upf3a* gene largely corrects the olfactory defect caused by complete loss of *Upf3b*. Second, the double-mutant mice were able to normally regenerate mOSNs (as measured by OE thickness) after chemical ablation, unlike single-mutant *Upf3b* mice. Remarkably, double-mutant mice were able to regenerate mOSNs as well as wild-type mice. Third, double mutant mice had nearly wild-type levels of HBC and mOSN markers, implying that loss of *both Upf3a* and *Upf3b* corrects maturation defects caused by loss of either of these genes alone. This suggests cellular mechanisms by which the olfactory defects (detected by weaning weight) are corrected by loss of both paralogs. For example, depletion and loss of UPF3A and UPF3B, respectively, may restore the appropriate balance of these two factors to restore normal HBC homeostasis. This, in turn, may correct differentiation defects, thereby allowing for the generation of normal numbers of mOSNs. Finally, the NMD substrates in the double-mutant mice are closer in level to that in wild-type mice than in *Upf3a*- or *Upf3b*-single mutant mice. This suggests a molecular mechanism for correction of the olfactory defects – loss of both *Upf3a* and *Upf3b* genes leads to partial restoration of a normal magnitude of NMD.

Together, these data strongly support the notion that defects resulting from complete loss of UPF3B can be rescued, at least partially, by loss of UPF3A. This supports hypothesis that these two proteins act oppositely of one another and that losing both factors can effectively cancel each other out.

Implications and Clinical Relevance of UPF3A

The prospect of UPF3A being a clinical target for patients that lack UPF3B is plausible according to what has been shown in my studies herein. One future experiment to test the efficacy of this approach would be to generate a *Upf3b-null* mouse with *Krt*-Cre driver mice and two *Upf3a*-floxed alleles and measure its behavior. Since the Cre is inducible by tamoxifen, it can be determined whether induced loss of *Upf3a* at different developmental time points is sufficient to “cure” defects.

While UPF3A is a good candidate target to treat UPF3B deficiency linked intellectual disability, it is not without its risks, as with any medical treatment. From the data obtained from the *Upf3a-cKO*, it seemed that there was a wide variety of transcripts that were down-regulated in response to UPF3A loss. It seems highly unlikely that such effects would not result in adverse reactions in certain tissues in the body. The brain, heart, and spleen all showed unique reactions to UPF3A haploinsufficiency, and it is difficult to predict what specific problems there could be. Another potential downside to depleting or inhibiting UPF3A as a means of therapy is it may lead to decreased stem cells that that could accelerate aging, or

make it more difficult to recover following injuries. The stem cells could decrease either due to exhaustion after numerous cell divisions, or possibly lost due to improper cell division. To follow-up on this, studies should be done to determine the effect of loss of *Upf3a*, *Upf3b*, or both, on longevity. Based on my studies in the OE, it would appear that inhibition of both UPF3A and UPF3B would maintain stem cells and thus not adversely affect longevity from this perspective. In contrast, inhibition of either UPF3A or UPF3B alone could lead to stem cell exhaustion that lead to complications in developmental processes that persist well into adulthood. It will be important to study ageing animals with deficiencies in UPF3A and/or UPF3B to define both molecular and cellular defects that control overall fitness during the ageing process.

Certain organ systems would probably fair better than others to “UPF3B therapy.” For example, the central nervous system would likely be less affected, as neurons divide very rarely, if at all. Other organ systems, such as those constantly needing to be replenished, are likely to be more susceptible to side effects. For example, gut mucosal cells could be greatly affected since they are constantly being renewed from stem cells. Their loss could result in very unpleasant symptoms as a result of degeneration within the gut. If these organs have much less cellular stress than their wild-type counterparts, it could be beneficial as the cells do not undergo apoptosis. This could also be deleterious if there is too little stress and this leads to accumulation of bad RNAs and proteins. As with all cellular processes, a delicate balance must be in place to ensure appropriate responses.

NMD is vital for surveillance of aberrant transcripts and for regulation of a subset of normal RNAs. While RNA surveillance is needed for the cell, it must also be regulated to ensure proper homeostasis. UPF3A and UPF3B could be evolution's answer to regulating and ensuring proper levels of RNA turnover, depending on cellular context and other developmental cues. Perhaps the etiology of the neurological defects that result from loss of UPF3B can be attributed to NMD being too inhibited, leading to accumulation of RNAs that need to be degraded for proper neurological development and function. Conversely, loss of UPF3A in male germ cells causes testis defects (unpublished observations from Eleen Shum in the Wilkinson laboratory). This may be because NMD needs to be repressed for proper spermatogenesis, as it allows the accumulation of crucial NMD target transcripts encoding key proteins for proper development and function of the testis. In the future, it will be important to test other organs for their requirement for NMD, as well as their sensitivity to NMD perturbation, including in response to drugs that inhibit UPF3A, UPF3B, or both. Given that NMD is upstream of a large network of process, the effects of hypo- or hyper-NMD can be more or less pronounced depending on cellular context.

IV:

Materials and Methods

Generation of Knockout Mouse Models

The *Upf3b*-null mouse model was generated by Lulu Huang (Huang et al. Manuscript in preparation). The *Upf3a*-null mouse was generated by Eleen Shum (Shum et al. manuscript in preparation). The double mutant mice were generated by breeding *Upf3a*-null and *Upf3b*-null mice together. The conditional knockout was bred by generating with floxed *Upf3a* alleles. Cre expression was driven by a *Krt5*-Cre, with specific expression in the HBCs of the OE. The *Krt5*-Cre mouse and *Rosa26*-LacZ mice were acquired from Jax laboratories.

RNA Isolation, Reverse Transcription, and qPCR

RNA was extracted using Trizol reagent (Life Technologies) and chloroform. After adding Trizol to cells or tissue samples, I added 1/5 of the volume of chloroform. The samples were centrifuged at maximum speed (16,000 rpm) for 20 minutes at 4° C. The aqueous layer was extracted and an equal volume of chloroform was added. This was centrifuged at maximum for speed 5 minutes at 4° C. The aqueous layer was extracted again and added with 1/10 sodium acetate and 2.5x 100% ethanol. This was let to precipitate for an hour at least. The samples were centrifuged at maximum speed for 20 minutes at 4° C. The supernatant was removed and an equal volume of 70% ethanol was added. The samples were centrifuged at maximum for speed 5 minutes at 4° C. The supernatant was completely removed and the pellet was re-suspended in nuclease free water. The RNA concentration was taken using a nanodrop. The 1ng of RNA was then put

into a 20μL reaction for reverse transcription (Bio-Rad). The cDNA was then used in PCR reactions with Sybr green dye for qPCR reactions.

Tissue Isolation and Fluorescent Staining

Mice were sacrificed using CO_2 gas and cervical dislocation. The OE was extracted and placed directly into formalin. The samples were fixed and de-calcified prior to paraffin embedding. After embedding, the samples were rehydrated. Antigen retrieval was performed. Samples were incubated with primary antibody diluted 1:100 in PBS with 10% BSA and 1% serum for at least overnight. Secondary antibodies were diluted 1:500 in PBS with 10% BSA and 1% serum for at least an hour. Samples were mounted using Vectashield reagent with DAPI (Vector labs).

Cell culture, transfection, and plasmids

P19 cells were cultured with MEMα media with 10% FBSP at 37° C.

P19 cells were transiently transfected with Lipofectamine 2000 reagent as described in the protocol (Invitrogen).

NMD activity was measured using an NMD reporter using Renilla luciferase reporters that were either PTC+ or PTC- with a firefly endogenous control (Boelz *et al.* 2006)

UPF3A mutants were cloned by the Gehring group as reported in Kunz *et al.* 2006

Western Blot

Protein samples were extracted from homogenized tissue using RIPA buffer with protease inhibitor. The concentrations were determined using a BSA standard curve. 20µg of protein was used per sample. Samples were run on SDS-PAGE gels for two hours. Proteins were transferred to a nitrocellulose blot overnight at 4° C. Blot was incubated with blocking solution. Primary antibodies were diluted 1:1000 in blocking solution and added to blots at least overnight. Secondary antibodies were diluted 1:5000 in blocking solution for at least an hour. Substrate was added and films were developed for visualization.

References

Addington, A. M., Gauthier, J., Piton, A., Hamdan F. F., Raymond, A., Gogtay, N., Miller, R., Tossell, J., Bakalar, J., Inoff-Germain, G., Gochman, P., Long, R., Rapoport, J.L., Rouleau, G.A. A novel frameshift mutation in UPF3B identified in brothers affected with childhood onset schizophrenia and autism spectrum disorders. Mol Psychiatry 16, 238–239 (2011).

Bozza, T., Vassalli A., Fuss S., Zhang J. J., Weiland B., Pacifico R., Feinstein P., Mombaerts P. Mapping of class I and class II odorant receptors to glomerular domains by two distinct types of olfactory sensory neurons in the mouse. Neuron 2, 220-233 (2009)

Carter, M. S., Li, S., Wilkinson M. F. A Splicing-dependent regulatory mechanism that detects translation signlas EMBO 21, 5965-5975 (1996)

Chan, W. K., Bhalla A. D., Le Hir, H., Nguyen, L. S., Huang, L., Gecz, J., Wilkinson, M. F. A UPF3-mediated regulatory switch that maintains RNA surveillance. Nat Struct Mol Biol 16, 747–753 (2009).

Chan, W. K., Huang, L., Gudikote, J. P., Chang, Y. F., Imam, J. S., Maclean, J. A., Wilkinson, M. F. An alternative branch of the nonsense-mediated decay pathway. EMBO J 26, 1820–1830 (2007).

Chang, Y.-F. F., Imam, J. S. & Wilkinson, M. F. The nonsense-mediated decay RNA surveillance pathway. Annu Rev Biochem 76, 51–74 (2007).

Chinen, M., Tani, T. Diverse functions of nuclear non-coding RNAs in eukaryotic gene expression. Front Biosci 17, 1402-1417 (2012)

Dalton R. P., Lyons D. B., Lomvardas, S. Co-opting the unfolded protein response to elicit olfactory receptor feedback. Cell 155, 321-332 (2013)

Demaria, S., Berke, A. P., Van Name, E., Heravian, A.m Ferreira, T., Ngai, J. Role of a ubiquitously expressed receptor in the vertebrate olfactory system. J Neuroscience 33, 15235-15247 (2010)

Fletcher R. B., Prasol M. S., Estrada, J., Baudhuin, A., Vranizan, K., Choi, Y. G., Ngai, J. p63 regulates olfactory stem cell self-renewal and differentiation. Neuron 72, 748-759 (2011)

Fletcher, R. B., Prasol M. S., Estrada J., Baudhuin A., Vranizan K., Choi Y. G., Ngai J. p63 regulates olfactory stem cell self-renewal and differentiation. Neuron 72, 748–759 (2011).

Guan, Q., Zheng, W., Tang, S., Liu, X., Zinkel, R. A., Tsui, K., W., Yandell, B. S., Culbertson, M. R. Impact of nonsense-mediated mRNA decay on the global expression profile of budding yeast. PLoS Genet 2, e203 (2006).

Haehner, A., Hummel, T., Reichmann, H. Olfactory loss in Parkinson's disease. Parkinsons. Disease 2011, 450939 (2011).

He, F., Li X., Spatrick P., Casillo R., Dong S., Jacobson A. Genome-wide analysis of mRNAs regulated by the nonsense-mediated and 5' to 3' mRNA decay pathways in yeast. Mol Cell 12, 1439–1452 (2003).

Huang, L. & Wilkinson, M. F. Regulation of nonsense-mediated mRNA decay. Wiley Interdiscip Rev RNA 3, 807–828 (2012).

Huang, L., Lou, C. H., Chan, W., Shum, E. Y., Shao, A., Stone, E., Karam, R., Song, H. W., Wilkinson, M. F. RNA homeostasis governed by cell type-specific and branched feedback loops acting on NMD. Mol Cell 43, 950–961 (2011).

Hwang, J. & Maquat, L. E. Nonsense-mediated mRNA decay (NMD) in animal embryogenesis: to die or not to die, that is the question. Curr Opin Genet Dev 21, 422–430 (2011).

Iwai, N., Zhou, Z., Roop, D. R. & Behringer, R. R. Horizontal basal cells are multipotent progenitors in normal and injured adult olfactory epithelium. Stem Cells 26, 1298–1306 (2008).

Jolly, L. A., Homan, C. C., Jacob, R., Barry, S. & Gecz, J. The UPF3B gene, implicated in intellectual disability, autism, ADHD and childhood onset schizophrenia regulates neural progenitor cell behaviour and neuronal outgrowth. Hum. Mol. Genet. ddt315– (2013).

Kadlec, J., Izaurralde, E., Cusak, S. The structural basis for the interaction between nonsense-mediated mRNA decay factors UPF2 and UPF3. Nature Structural & Molecular Biology 11, 330-337 (2004)

Karam, R., Wengrod, J., Gardner, L. B., Wilkinson, M. F. Regulation of nonsense-mediated mRNA decay: implications for physiology and disease. Biochim Biophys Acta. 1829, 624-633 (2013)

Kervestin, S. & Jacobson, A. NMD: a multifaceted response to premature translational termination. Nat Rev Mol Cell Biol 13, 700–712 (2012).

Kulahin, N. & Walmod, P. S. The neural cell adhesion molecule NCAM2/OCAM/RNCAM, a close relative to NCAM. Adv Exp Med Biol 663, 403–420 (2010).

Kunz, J. B., Neu-Yilik, G., Hentze, M. W., Kulozik, A. E., Gehring, N. H. Functions of hUPF3a and hUPF3b in nonsense0mediated mRNA decay and translation RNA 6, 1015-1022 (2006)

Laumonnier, F., Shoubridge C, Antar C, Nguyen LS, Van Esch H, Kleefstra T, Briault S, Fryns JP, Hamel B, Chelly J, Ropers HH, Ronce N, Blesson S, Moraine C, Gécz J, Raynaud M. Mutations of the UPF3B gene, which encodes a protein widely expressed in neurons, are associated with nonspecific mental retardation with or without autism. Mol. Psychiatry 15, 767–76 (2010).

Lelivelt, M. J. & Culbertson, M. R. Yeast Upf proteins required for RNA surveillance affect global expression of the yeast transcriptome. Mol Cell Biol 19, 6710–6719 (1999).

Leung, C. T., Coulombe, P. A. & Reed, R. R. Contribution of olfactory neural stem cells to tissue maintenance and regeneration. Nat Neurosci 10, 720–726 (2007).

Logan, D. W., Brunet, L. J., Webb, W. R., Cutforth, T., Ngai, J., Stowers, L. Learned recognition of maternal signature odors mediates the first suckling episode in mice. Cell Press 21, 1998-2007 (2012).

Lou, C. H., Shao A., Shum E. Y., Espinoza J. L., Huang L., Karam R., Wilkinson M.F., Posttranscriptional Control of the Stem Cell and Neurogenic Programs by the Nonsense-Mediated RNA Decay Pathway. Cell Reports (2014).

Lykke-Andersen, J., Mei-Di, S., Steitz, J. A. Human Upf proteins target an mRNA for nonsense-mediated decay when bound downstream of a termination codon. Cell 103, 1121-1131 (2000).

Mackay-Sim, A., Kittel, P. Cell dynamics in the adult mouse olfactory epithelium: a quantitative autoradiographic study J Neuroscience 11, 979-984 (1991)

Melero, R., Buchwald, G., Castano, R., Raabe, M., Gil, D., Lazaro, M., Urlaub, H., Conti, E., Llorca, O. The cryo-EM structure of UPF-EJC complex shows UPF1 posed towards the RNA 3’ end Nature Structural & Molecular Biology 19, 498-505 (2012)

Mendell, J. T., Sharifi, N. A., Meyers, J. L., Martinez-Murillo, F. & Dietz, H. C. Nonsense surveillance regulates expression of diverse classes of mammalian transcripts and mutes genomic noise. Nat Genet 36, 1073–1078 (2004).

Nguyen, L. S. Jolly L., Shoubridge C., Chan W. K., Huang L., Laumonnier F., Raynaud M., Hackett A., Field M., Rodriguez J., Srivastava A. K., Lee Y., Long

R., Addington A. M., Rapoport J. L., Suren S., Hahn C. N., Gamble J., Wilkinson M. F., Corbett M. A., Gecz J. Transcriptome profiling of UPF3B/NMD-deficient lymphoblastoid cells from patients with various forms of intellectual disability. Mol. Psychiatry 17, 1103–15 (2012).

Nguyen, L. S., Kim H. G., Rosenfeld J. A., Shen Y., Gusella J. F., Lacassie Y., Layman L. C., Shaffer L. G., Gécz J. Contribution of copy number variants involving nonsense-mediated mRNA decay pathway genes to neuro-developmental disorders. Hum. Mol. Genet. 22, 1816–1825 (2013).

Nicholson, P. Yepiskoposyan H., Metze S., Zamudio Orozco R., Kleinschmidt N., Mühlemann O. Nonsense-mediated mRNA decay in human cells: mechanistic insights, functions beyond quality control and the double-life of NMD factors. Cell Mol Life Sci 67, 677–700 (2010).

Oren, Y. S., McClure M. L., Rowe S. M. , Sorscher E. J., Bester A. C., Manor M., Kerem E., Rivlin J., Zahdeh F., Mann M., Geiger T., Kerem B. The unfolded protein response affects readthrough of premature termination codons EMBO Mol Med 6, 685-701 (2014)

Piras, E., Franzen A., Fernandez, E. L., Bergstrom, U., Raffalli-Mathieu, F., Lang, M., Brittebo, E. B. Cell-specific expression of CYP2A5 in the mouse respiratory tract: effects of olfactory toxicants. J. Histochem Cytochem 51, 1545-1555 (2003)

Ramani, A. K., Nelson A. C., Kapranov P., Bell I., Gingeras T. R., Fraser A. G. High resolution transcriptome maps for wild-type and nonsense-mediated decay-defective Caenorhabditis elegans. Genome Biol 10, R101 (2009).

Rebbapragada, I. & Lykke-Andersen, J. Execution of nonsense-mediated mRNA decay: what defines a substrate? Curr Opin Cell Biol 21, 394–402 (2009).

Rehwinkel, J., Letunic, I., Raes, J., Bork, P. & Izaurralde, E. Nonsense-mediated mRNA decay factors act in concert to regulate common mRNA targets. RNA 11, 1530–1544 (2005).

Rupp, C. I. Olfactory function and schizophrenia: an update. Curr Opin Psychiatry 23, 97–102 (2010).

Sakaki, K., Kaufman, R. J. Interaction between quality control systems for ER protein folding and RNA biogenesis. Worm 2(2): e23005 (2013)

Schoenberg, D. R. & Maquat, L. E. Regulation of cytoplasmic mRNA decay. Nat. Rev. Genet. 13, 246–59 (2012).

Scholzen, T., Gerdes, J. The Ki67 protein: from the known to the unknown. J Cell Physiology 3, 311-322 (2000)

Serin, G., Gersappe, A., Black, J. D., Aronoff, R., Maquat, L. E. Identification and characterization of human orthologues to Saccharomyces cerevisiae Upf2 protein and Upf3 protein (Caenorhabditis elegans SMG-4). Mol Cell Bio 1, 209-223 (2001)

Smith, C., Steitz J. A. Classification of gas5 as a Multi-Small-Nucleolar-RNA (snoRNA) Host Gene and a Member of the 5′-Terminal Oligopyrimidine Gene Family Reveals Common Features of snoRNA Host Genes. Mol Cell Bio 12, 6897-6909 (1998)

Szyszka, P., Sharp, S. I., Dedman, A., Gurling, H. M. D. & McQuillin, A. A nonconservative amino acid change in the UPF3B gene in a patient with schizophrenia. Psychiatr. Genet. 22, 150–1 (2012).

Tarpey, P. S. Raymond F. L., Nguyen L. S., Rodriguez J., Hackett A., Vandeleur L., Smith R., Shoubridge C., Edkins S., Stevens C., O'Meara S., Tofts C., Barthorpe S., Buck G., Cole J., Halliday K., Hills K., Jones D., Mironenko T., Perry J., Varian J., West S., Widaa S., Teague J., Dicks E., Butler A., Menzies A., Richardson D., Jenkinson A., Shepherd R., Raine K., Moon J., Luo Y., Parnau J., Bhat S. S., Gardner A., Corbett M., Brooks D., Thomas P., Parkinson-Lawrence E., Porteous M. E., Warner J. P., Sanderson T., Pearson P., Simensen R. J., Skinner C., Hoganson G., Superneau D., Wooster R., Bobrow M., Turner G., Stevenson R. E., Schwartz C. E., Futreal P. A., Srivastava A. K., Stratton M. R., Gécz J. Mutations in UPF3B, a member of the nonsense-mediated mRNA decay complex, cause syndromic and nonsyndromic mental retardation. Nat Genet 39, 1127–1133 (2007).

Tarutani, M., Itami, S., Okabe, M., Ikawa, M., Tezuka, T., Yoshikawa, K., Kinoshita, T., Takeda, J. Tissue-specific knockout of the mouse Pig-a gene reveals important roles for GPI-anchored proteins in skin development. PNAS 14, 7400-7405 (1997)

Tsuboi, A., Miyazaki, T., Imai, T., Sakano, H. Olfactory sensory neurons expressing class I odorant receptors converge their axons on an antero-dorsal domain of the olfactory bulb in the mouse. Euro J Neuroscience 6, 1436-1444 (2006)

Tycowski, K. T., Shu, M. D., Steitz, J. A. A mammalian gene with introns instead of exons generating stable RNA products. Nature 6564, 464-466 (1996)

Whitman, M. C. & Greer, C. A. Adult neurogenesis and the olfactory system. Prog. Neurobiol. 89, 162–75 (2009).
Wittkopp, N., Huntzinger E., Weiler C., Sauliere J., Schmidt S., Sonawane M., Izaurralde E. Nonsense-mediated mRNA decay effectors are essential for zebrafish embryonic development and survival. Mol Cell Biol. 13, 3517-3528 (2009)

Wittmann, J., Hol, E. M. & Jack, H. M. hUPF2 silencing identifies physiologic substrates of mammalian nonsense-mediated mRNA decay. Mol Cell Biol 26, 1272–1287 (2006).

Yepiskoposyan, H., Aeschimann F., Nilsson D., Okoniewski M., Mühlemann O. Autoregulation of the nonsense-mediated mRNA decay pathway in human cells. RNA 12, 2108-2118 (2011)

Yoshida, H., Matsui T., Yamamoto A., Okada T., Mori K. XBP1 mRNA is induced by ATF6 and spliced by IRE1 in response to ER stress to produce a highly active transcription factor. Cell 107, 881-891 (200)

Zhang, X., Firestein, S. The olfactory receptor gene superfamily of the mouse. Nature Neuroscience 2, 124-133 (2002)